Published online: December 30, 2020

IMR Press

Original Research

Small-world EEG network analysis of functional connectivity in developmental dyslexia after visual training intervention

Juliana A. Dushanova[1,*] and Stefan A. Tsokov[1]

[1]*Institute of Neurobiology, Bulgarian Academy of Sciences, 23 Acad. G. Bonchev St., 1113, Sofia, Bulgaria*

*Correspondence: juliana@bio.bas.bg (Juliana A. Dushanova)

DOI:10.31083/j.jin.2020.04.193

Aberrations in functional connectivity in children with developmental dyslexia have been found in electroencephalographic studies using graph analysis. How training with visual tasks can modify the functional semantic network in developmental dyslexia remains unclear. We investigate local and global topological properties of functional networks in multiple EEG frequency ranges based on a small-world propensity method in controls, pre- and post-training dyslexic children during visual word/pseudoword processing. Results indicated that the EEG network topology in dyslexics before the training was more integrated than controls, and after training - more segregated and similar to that of the controls in the theta (θ: 4-8), alpha (α: 8-13), beta (β1: 13-20; β2: 20-30), and gamma (γ1: 30-48; γ2: 52-70 Hz) bands for three graph measures. The pre-training dyslexics exhibited a reduced strength and betweenness centrality of the left anterior temporal and parietal regions in the θ, α, β1 and γ1-frequency bands, compared to the controls. The simultaneous appearance of hubs in the left hemisphere (or both hemispheres) at temporal and parietal (α-word/γ-pseudoword discrimination), temporal and middle frontal cortex (θ, α-word), parietal and middle frontal cortex (β1-word), parietal and occipitotemporal cortices (θ-pseudoword), identified in the EEG-based functional networks of normally developing children were not present in the networks of dyslexics. The hub distribution for dyslexics in the θ, α, and β1 bands became similar to that of the controls. The topological organization of functional networks and the less efficient network configuration (long characteristic path length) in dyslexics compared to the more optimal global organization in the controls was studied for the first time after remediation training.

Keywords

EEG; functional connectivity; developmental dyslexia; frequency oscillations; connectome; graph theory; neural computation

1. Introduction

Developmental dyslexia (DD) is a childhood disorder related to reading, writing, spelling, and learning inability of these skills, despite normal intellectual abilities. Early diagnosis of dyslexia (Stein, 2014) can prevent specific problems of children with developmental dyslexia related to their social and mental development. Therefore, some actions are needed to prevent cognitive disorders complicating the childhood of children with dyslexia. Although developmental dyslexia has been studied extensively on a behavioral level (Benassi et al., 2010; Boets et al., 2011; Cornelissen et al., 1998; Demb et al., 1998; Pammer and Wheatley, 2001; Sperling et al., 2005; Stein, 2014), there is no consensus regarding its causes. According to the 'dual route' model, the words can be read either by lexical or sub-lexical route (Coltheart et al., 2001). In the lexical route, the words are directly recognized as lexicon members and associated with verbal semantic representations, when they are familiar, automatically identified by their visual form (Coltheart et al., 2001). In the sub-lexical route, based on grapheme to phoneme correspondence rules for unfamiliar words, the word is broken down into its constituent letters and corresponding phonemes (Coltheart et al., 2001). Impairment in either of these routes will result in a characteristic pattern of reading difficulties (Castles and Coltheart, 1993). When the children's deficits are in phonological skills (so-called phonological dyslexia, Funnell, 1983), they probably use the lexical route to compensate for the sub-lexical route (Siegel, 1993), as well as naming irregular words well, but not pseudo-words (nonsense words). When the problems are in the lexical route, the sub-lexical route is used (Ebrahimi et al., 2019). Then, the pseudo-words could be processed, but not the irregular words (Hodges and Patterson, 2007; Patterson and Hodges, 1992; surface dyslexia).

Different behavioral studies of dyslexics have found various deficits in the sensitivity to a coherence motion perception (Benassi et al., 2010; Boets et al., 2011), velocity discrimination (Demb et al., 1998; Eden et al., 1996), motion direction encoding (Cornelissen et al., 1998; Stein, 2014), contrast sensitivity to stimuli with low-/high-spatial frequency in external noise (Pammer and Wheatley, 2001; Sperling et al., 2005). These deficits are selectively associated with low accuracy or slow performance on reading sub-skills (Wilmer et al., 2004), problems with clearly seeing letters and their order, orienting and focusing on visual-spatial attention (Lalova et al., 2018; Stein, 2014). The deficits in the magnocellular pathway, established by the coherent motion perception, were associated with letter decoding disability (Cornelissen et al., 1998; Facoetti et al., 2003; Sperling et al., 2003).

Journal of Integrative Neuroscience

The magnocellular system is the visual input to the dorsal pathway that mediates motion perception and object localization (Goodale and Westwood, 2004) due to the projections to the visual motion-sensitive area and the posterior parietal cortex. For the reading, the dorsal pathway has a major role in directing visual attention and control of eye movements (Stein, 2014). The efficacy of intervention efforts has also been studied (Chouake et al., 2012; Lalova et al., 2019; Lawton, 2011, 2016; Lawton and Shelley-Tremblay, 2017; Qian and Bi, 2015). After visual magnocellular training, children with reading difficulties improved coherent motion detection, saccadic eye movements, as well as reading accuracy and visual errors (Ebrahimi et al., 2019). By detecting progressively faster movements in the coherent motion discrimination, the lexical decision and reading accuracy improved at the magnocellular system's higher visual levels (Chouake et al., 2012). The phonological errors for dyslexic readers decreased after magnocellular intervention by figure-ground movement discrimination (Lawton, 2016; Lawton and Shelley-Tremblay, 2017). The reduction in phonological errors and visual timing deficits, the improvements in reading fluency, attention, phonological processing, and working memory result from an improvement in the dorsal stream's functioning levels. The detection of abnormal functioning brain regions and changed communication with other brain regions in dyslexia is directed to create early diagnosis methods (Stein, 2014). Generally, due to anterior and middle temporal lobe deficits, affecting primary ventral, occipitotemporal, lexical route, children with severe phonological disabilities rely more on ventral (Funnell, 1983; occipitotemporal lexical) brain regions, whereas other dyslexic readers with less pronounced phonological deficits use more the dorsal (occipitoparietal sublexical) route. The dorsal stream consists of three pathways with projections to the prefrontal and premotor cortices, with a major projection to the medial temporal lobe with direct and indirect courses through the posterior cingulate and retrosplenial cortices with reciprocal projections to the visual cortex (Kravitz et al., 2011). The ventral stream is a multisynaptic pathway with projections from the striate cortex to the anterior temporal part in the inferior temporal cortex, with a further projection from the rostral inferior temporal to the ventral prefrontal cortex. When the lexical route has deficits, as in dyslexics with less pronounced phonological deficits, partial compensation appears to be possible by over-recruitment of the slower, attention dependent, sublexical one. Therefore, neuropsychological evidence for the dyslexic groups supposes that partially distinct neural substrates as a dorsal and a ventral route, respectively, underlie sublexical and lexical processes (Ebrahimi et al., 2019; Stein, 2014). A lexicosemantic route involves the left basal temporal language area, the posterior part of the middle temporal gyrus, and the inferior frontal gyrus, and a sublexical route involving the left-lateralized superior temporal area, supramarginal gyrus, and the opercular part of the inferior frontal gyrus (Jobard et al., 2003). Nevertheless, controversies still exist about the anatomical substrates involved in lexical and sublexical reading routes (Jobard et al., 2003; Mechelli et al., 2003). Neuroplastic mechanisms and synaptic reorganization that mediate the training effects in functionally implement visual rehabilitation (Magosso et al., 2017) among uni-sensory areas strengthen due to learning mechanisms, which stimulate the maturation in typically developing children (Cuppini et al., 2017) and the multisensory development emerging quite late during development (Dekker et al., 2015). The training stimulates not only compensations in the visual and oculomotor functioning (Magosso et al., 2017). Still, it may further contribute to the multisensory integration in semantic memory and semantic link content with lexical language features (Ursino et al., 2015).

It has been established that human semantic knowledge is supported by large brain networks, encompassing many different brain regions and coordinated by a central hub or hubs. Among the candidates for these semantic hubs are the anterior temporal lobe (ATL), the posterior inferior parietal lobe (particularly the angular gyrus, AG), the middle temporal gyrus (MTG) and the inferior frontal gyrus (IFG) (Binder et al., 2009; Farahibozorg et al., 2019). The dynamics of the heteromodal semantic network and the roles of the hubs have been investigated by neuro-computational modeling (Tomasello et al., 2017) and experimentally using visually presented words (Farahibozorg et al., 2019). The question is whether methods, based on the graph theory, can be used as a screening test for developmental dyslexia, and whether this approach can shed light on the neurophysiological causes for the effect of visual nonverbal training (Ebrahimi et al., 2019; Lalova et al., 2019; Lawton, 2011; Wilmer et al., 2004)? The hypothesis is that the visual training intervention on children with dyslexia can lead to changes in the EEG-based functional networks, making them more similar to controls. We also hypothesize that the training, affecting the dorsal pathway, may influence the semantic network's functioning related to the word meanings (semantics) or their structure (syntax).

The study's first goal is to prove that network-level statistics is a useful tool to screen developmental dyslexia, comparing controls and dyslexics by focusing on their connectivity networks using the small-world propensity (SWP) algorithm applied to electroencephalogram (EEG) data. The second goal is to demonstrate that visual nonverbal training can help reduce the brain networks' abnormality related to developmental dyslexia by network-level statistics between the pre- and post-training groups with dyslexia (cf. Taskov and Dushanova, 2020).

2. Materials and methods

2.1 Study design

A longitudinal study was conducted in the schools that involved repeated observations of children with developmental dyslexia over a long period. In this observational study with the exposure of visual intervention in non-trial research, the dyslexics are then followed out over time to observe the outcome from the visual training and evaluate the extent to which the visual tasks contribute to the alteration of this childhood disorder.

2.2 Participants

Reliable electrophysiological data were obtained from forty-three children: 22 children with dyslexia (12 boys and 10 girls) and 21 normal children (11 boys and 10 girls). The age range for both groups was 8-9 years old. All children and their parents gave informed consent for an EEG following the Helsinki Declaration. The Ethics Committee approved the Institute of Neurobiology study, the Institute for Population and Human Studies, BAS, the State Logopedic Center, and the Ministry of Education and Science. All participants in the study spoke Bulgarian as

their first language. All children were right-handed. The handedness was assessed by a classification of hand preference (Annett, 1970). All participants had non-verbal intelligence scores of 98 or higher (Raven et al., 1998). All children had normal or corrected-to-normal vision. The controls were paid 100 Bulgarian Lev for participating.

The children underwent a series of tests, including neuropsychological tests (Raichev et al., 2005), a DDE-2 test battery for the evaluation of developmental dyslexia (Matanova and Todorova, 2013; Sartori et al., 2007), psychometric tests for the evaluation of phonological awareness, tests for the evaluation of reading and writing skills (Kalonkina and Lalova, 2016), Girolami-Boulinier's "Different Oriented Marks" nonverbal perception test (Girolami-Boulinier, 1985; Yakimova, 2004), and Raven's Progressive Matrices test for nonverbal intelligence (Raven et al., 1998). In the dyslexic group were included children with reading difficulties combined with below-norm performance in either speed or accuracy below one standard deviation from age-matched standardized control data in reading subtests in the DDE-2 battery (word list reading, pseudoword list reading, choosing the correct meaning of a word, search for misspellings of words; writing of word/pseudoword in dictation), as well as in the test battery "Reading abilities" (identifying the first sound in a heard word and omitted it in the word, fragmentation of the word in syllables and missed the last syllable, text reading, dictation of sentences filling in a missing compound word). The control participants included age-matched children with the same socio-demographical background as the dyslexic group. There was no dyslexia or co-occurring language disorders confirmed by within-norm performance in speed and accuracy in reading. The results are shown in Table S1.

2.3 Experimental paradigm

The participants were exposed to two types of visual stimuli (Fig. 1), presented on a laptop with a screen resolution of 1920 × 1080 pixels and a refresh rate of 60 Hz at a distance of 57 cm from the observer. The stimuli stayed on the computer screen for 800 ms and consisted of multi-syllabic (2/3-syllables with 5.4 ± 0.7 letters) words and pseudowords, presented in pseudo-random order. The stimulus duration was chosen according to the mean duration of their aloud-related words with the same content (0.731 ± 0.15 ms) and pseudowords with distorted content of the same stimuli (mean duration 0.757 ± 0.16 ms). The font was Microsoft Sans Serif (black letters on a white background), and each letter had an angular size of about 1 deg. The selected words were age-appropriate for the children and encompassed the following parts of the speech: nouns (10), adjectives (2), verbs (12), numerals (2), prepositions (2), adverbs (8), and pronouns (4). The pseudowords were derived from the words by replacing all the vowels. The words were selected with a different frequency of use, balanced according to their frequency characteristics - low and high frequency. The Frequency Dictionary is created based on a hundred thousand Bulgarian words from conversational language (the 100 000 words were divided into 5 subgroups of 20 000 words each). According to the frequency of use, each word is assigned a certain rank. The smaller the rank, the more often the word is used. The numerator in the frequency indicates how often a particular word appears in the whole text group. Simultaneously, the denominator shows the number of subgroups this word appears in the maximum number is 5 (Nikolova, 1987). The words with a high frequency were from 387/5 to 138/5 and a corresponding rank of 46 to 110.5, while those with an average frequency of 88/5 to 40/5 and a rank of 150 to 273, as well the words with a low frequency - from 13/3 to 25/5 and rank from 368.5 to 624.5. The words in the task had no orthographic and phonological neighborhoods.

The stimuli were presented in two to four blocks during daily EEG experimental sessions. Each block contained 40 words and 40 pseudowords (Fig. 1). For the first two blocks, stimuli were randomized and presented once. The presentation of all stimuli was repeated in blocks 3 and 4 to increase the number of trials and consequently signal to noise ratio. Participants were asked to blink only during the interstimulus interval (1.5-2.5 s) to prevent artifacts in the EEG records during the words/pseudowords stimuli. The participants were instructed to push a button with the right hand when seeing a word and push a different button with the left hand when the stimulus was a pseudoword. Two behavioral parameters were evaluated for each child: the percentage of correctly identified words/pseudowords and the reaction time. To examine whether visual perceptional training can influence the neural semantic network of the children with developmental dyslexia, we recorded EEG session during visual word/pseudoword task one month later after the three-month training with five visual program interventions. Hence, irrespective of the word/pseudoword task, the experimental group received an intensive procedure with training tasks, presented in an arbitrary order and divided twice a week into individual sessions lasting 45 minutes over three months. This long term period does not enable the children with developmental dyslexia to memorize information about the word/pseudoword task performed before the training period.

The visual perceptual training comprised five visual program interventions that do not include any direct phonological input on the children with developmental dyslexia (Fig. 1). The training program, based on direction discrimination of coherent vertical motion (Benassi et al., 2010; Boets et al., 2011), stimulated the magnocellular function. Coherent vertical motion of white dots in randomly moving elements with a size of 0.1 deg was presented within a circle (diameter 20 deg) on a black screen at a viewing distance of 57 cm for 200 ms. The velocity of the moving dots was 4.4 deg/s. The coherent motion threshold was 50% of the randomly moving dots. The inter-stimulus interval (ISI) was 1.5-2.5 sec. The child was instructed to press a button with the left hand for the upwards dots movement and press a different button with the right hand when the stimulus moves downwards.

The training program, based on velocity discrimination (Joshi and Falkenberg, 2015), induced changes in the MT/V5 brain area. Two pair circular stimuli with radial moving white dots' elements from center to periphery of optical flow (a diameter of 10 deg) appeared sequentially one after other on a screen. Each stimulus pair's first item was always with a constant slow speed (4.5 deg/s). The second item in the pair of stimuli had a speed of the flow (5.0 deg/s) close to that of the first stimulus (4.5 deg/s) or with a higher (5.5 deg/s). The first item appeared for 300 ms, and after 500 ms, the second item in the stimulus pair appeared for 300 ms at a viewing distance of 57 cm. The ISI was 1.5-3.5 sec. The instruction was to press a key with the right hand when the pair's

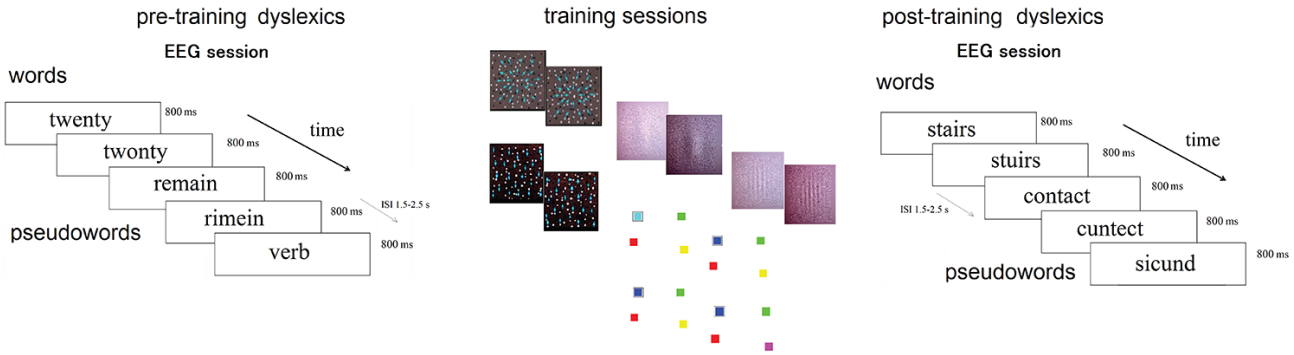

Fig. 1. The first and third block-diagrams are tasks for visual discrimination of words/pseudowords during the EEG sessions, recording before and after training. The words/pseudowords were in Bulgarian in the original experiment. The words are shown translated into English. The second block-diagrams present the training nonverbal tasks.

speed was slow or another key with a left hand when the second stimulus in the pair had a higher speed than the first stimulus's constant speed.

Low-contrast discrimination of low-spatial frequency sinusoidal gratings (2 cycles per degree of visual angle, (cpd)) and high-temporal frequencies (counter-phase flicker at 15 reversals/s), vertically flicking in external noise region (11 × 11 cm), maximally activated magnocellular cells (Pammer and Wheatley, 2001; Sperling et al., 2005). The stimuli were presented in a center on a gray screen with a fixation cross. The contrast levels were 6% and 12% of the contrast threshold, defined in previously psychophysical experiments (Lalova et al., 2018). Gratings with different contrasts were presented in a pseudo-randomized sequence with an ISI of 1.5-3.5 sec. The stimulus was subtended 2.7 × 2.7 deg visual angle at a viewing distance of 210 cm on a screen for 200 ms. Pressing the corresponding button with a left hand, the child discriminated low-contrast stimulus, with a right hand - the sinusoidal grating with high contrast. High-contrast discrimination of high spatial frequency sinusoidal gratings (10 cpd), vertically flicking in external noise region with contrast levels of 3% and 6% of defined contrast threshold (Lalova et al., 2018), were used to increase parvocellular type activity. The other parameters of the task and the child's requirements were the same as the previous task.

The visual-spatial attentional task with high peripheral processing demands was to search and track either color change or color preservation of a square in a cue (Ross-Sheehy et al., 2011). The cue was a black frame for 300 ms in either left or right visual field on a white screen, before the square color array (each with size 3 × 3 deg). A color square has appeared in the cue for 200 ms horizontally or vertically in an arranged color-array of four squares. The cue remained on the screen during the presentation of the color-array. The child had to compare the square color in the cue with the previous one presented in it on the screen at a viewing distance of 57 cm from the child. The adjacent squares in the array changed their colors in every presentation. The ISI was 1.5-2.5 sec. The child pressed a key on a computer keyboard with a left hand when two consecutive colors in the cue were the same, and with the right hand - when they were different. The number of correct answers and the reaction time was reported in the training programs with 40 trials in each condition and task. Thresholds of parameters and program designs were described in previous works (Lalova et al., 2019).

2.4 EEG recording and signal pre-processing

The EEG was recorded with an in-house developed 40-channel Wi-Fi EEG system using dry EEG sensors (each sensor is a matrix with 16 golden pins in a star-shaped configuration, Brain Rhythm Inc., Taiwan; Liao et al., 2011). Reference sensors were placed to both processus mastoidei and a ground sensor - on the forehead. The sensors were positioned on the head according to the international 10-20 system: F3-4, C3-4, T7-8, P3-4, O1-2; Fz, Cz, Pz, Oz, and additional positions according to the 10-10 system: AF3-4, F7-8, FT9-10, FC3-4, FC5-6, C1-2, C5-6, CP1-2, CP3-4, TP7-8, P7-8, PO3-04, PO7-08. The skin impedance was controlled to be less than 5 kΩ. The sampling EEG rate was 250 Hz. The continuous EEG data was band-pass filtered into the following frequency bands: δ = 1.5-4; θ = 4-8; α = 8-13; $\beta 1$ = 13-20; $\beta 2$ = 20-30; $\gamma 1$ = 30-48; $\gamma 2$ = 52-70 Hz. The data was then segmented into trials that time-locked to the stimulus onset, each with a duration of 800 ms. Trials in which the EEG exceeded ± 200 μV were rejected as containing artifacts. We verified the signal to noise ratio (SNR) of the grand average stimuli evoked-related potentials (ERPs) (Dushanova and Christov, 2013). The SNR criterion takes into account the noise around the ERP. SNRs were calculated using:

$$\mathrm{SNR} = \mathrm{A}/\left(2 \times \mathrm{SD}_{\mathrm{noise}}\right) \quad (1)$$

where the amplitude A is the peak-to-peak voltage of the mean ERP and SD_{noise} is the standard deviation of the noise (ε), which is obtained by subtracting the mean from each individual visual ERP. For a given single electrode, ϵ is just the collection of residuals, when the mean visual ERP is subtracted from each individual ERP and SD_{noise} is the standard deviation over this collection. Cleaned EEGs were filtered (bandpass: 1-70 Hz; notch filter: 50 Hz). Only trials with correct responses and high SNR were included in the analysis. After artifact rejection, the mean number of trials per condition was 30 when averaging all correct trials over subjects. The subject with the smallest number of artifact-free and correct trials provided 20 segments per condition.

2.5 Functional connectivity

The functional connectivity for all possible pairs of electrodes was determined using the Phase Lag Index (PLI) (Stam et al., 2007; Vinck et al., 2011). This was done separately for each frequency band between the two-time series. The PLI gives information about the phase synchronization of two signals, i.e., if one signal lags behind the other, by measuring the asymmetry of the distribution of their instantaneous phase differences. The instantaneous phases can be calculated from the analytical signal based on the Hilbert transform. The PLI can have values between 0 and 1. A value of 0 indicates that the two signals are not phase-locked (or that their phase difference is centered on 0 mod π), whereas a PLI of 1 means that they are perfectly phase-locked with a phase difference different from 0 mod π. PLI does not depend on the signal's amplitude and is less sensitive to volume conduction in the brain and spurious correlations because of common sources (Stam et al., 2007; Vinck et al., 2011).

2.6 Small-world propensity (SWP)

Often brain networks are studied in terms of segregation and integration. Segregation reflects the brain's ability to process specific information locally, i.e., within a brain region or an interconnected group of adjacent regions. In contrast, integration can combine information from different brain regions (Cohen and D'Esposito, 2016). Graph measures can characterize brain network integration and segregation. Graph theory describes networks as a set of nodes and their connections (links, edges) based on statistical calculations over connectivity strengths and node-node neighboring. The small world is the ratio of these measures, such as the clustering coefficient, the global efficiency and the characteristic path length (Rubinov and Sporns, 2010). Their sensitivity to many parameters, such as the number of connections in the network or their density, the number of nodes, the distribution of weights, makes it difficult to compare them between different EEG-based networks. New approaches have been proposed to solve these problems, one of which is the small-world propensity (SWP) method. The SWP is a metric from the Graph theoretical analysis that provides an objective assessment of small-world structure in EEG-based networks with different densities, taking into account variations in network density (Muldoon et al., 2016). SWP can quantify the degree of small-world structure between different networks and compare the topological network structure between specific groups using network density.

2.6.1 Global measures

The functional connectivity in the EEG-based networks, calculated using the PLI between each channel, can construct an adjacency matrix. Each row and each column represent a sensor, i.e., a graph that connects all its nodes (channels). Some authors have proposed the use of the method of the small-world propensity (Muldoon et al., 2016) to assess unbiased small-world structure in real-word networks with varying densities to avoid the problem with methodological limitations in the comparison of different functional networks, observed in other network-based methods of the graph theory (Bassett and Bullmore, 2017). Disadvantages of these statistics are dependent on network density and neglect critical variables such as the strengths of connections between nodes, limiting their ability to diagnose and compare small-world structure in different EEG functional networks at different development times. Different age-related maturation processes are a class of weighted networks (Medaglia et al., 2015; Tsujimoto, 2008), where the strong and weak connections differentially contribute to overall network function (Bassett et al., 2012). The weak connections, identified recently as potential biomarkers in pathologies (Bassett et al., 2012), have been ignored because of commonly applied thresholding techniques. The network statistic (SWP) is sensitive to the density and strengths of functional connections between nodes.

The small-word propensity (SWP) is denoted by ϕ defines the properties of the small world of weighted networks by comparing the clustering coefficient and the characteristic path length of a network using regular lattice and random graphs that have the same number of nodes and the same probability power distribution of degrees over all nodes in the network (Muldoon et al., 2016). The SWP quantifies the deviation of the characteristic path length (ΔL) of the observed network (*Lobs*) and the clustering coefficient (ΔC of *Cobs*) from its null model as a lattice and random network:

$$\begin{gathered} \phi = 1 - \left(\left(\Delta C^2 + \Delta L^2\right)/2\right)^{1/2} \\ \Delta C = (\text{Clatt-Cobs})/(\text{Clatt-Crand}) \\ \text{and } \Delta L = (\text{Lobs-Lrand})/(\text{Llatt-Lrand}) \end{gathered} \tag{2}$$

where *Clatt* is the clustering coefficient of the null model of a lattice network and *Crand* is the clustering coefficient of the null model of a random network, respectively; *Llatt* and *Lrand* are the characteristic path lengths of the lattice and random networks.

The characteristic path length L is determined by the average minimum number of edges between all pairs of nodes, while the clustering coefficient C is determined by the number of triangles around a node relative to the number of all node's neighbors (Boccaletti et al., 2006; Onnela et al., 2005), which is related to brain segregation (Bullmore and Sporns, 2009; Rubinov and Sporns, 2010).

To calculate ϕ in the EEG network, it is necessary to determine the appropriate reference random network (*Crand, Lrand)* and lattice network (*Clatt*, *Llatt)*. In these models, nodes located closer in the EEG network are assumed to have a higher strength of connections between nodes and stronger edges than nodes located far in the network. A weighted lattice network is a model that is constructed by arranging the weights of the observed edges with the highest weight being assigned to edges corresponding to the smallest Euclidean distance between the nodes since the weight of the edge is reciprocally proportional to the physical distance between the nodes. The observed edge weights are ranked by decreasing strength, where the connections with N highest weights are randomly distributed among the edges representing a unit distance of one-dimensional lattice. The next N-1 edges of the highest weights are distributed among the lattice's edges corresponding to a two-dimensional lattice. This continues to proceed until the total number of edges in the real-world network has been placed in the lattice. After building the lattice, the edges are weighted by a distance such that close edges have a higher strength than distant edges. The connections with the highest strength in the lattice network have been distributed along with the diagonal adjacency matrix. The lattice network is characterized by a high clustering coefficient and low characteristic path length. When the deviation

of the clustering coefficient from its null model is maximal, the network is rewired. The random network is created by randomly distributed weighted edges between N nodes. The shortest path between them is small, and the connections are randomly assigned throughout the matrix. The clustering coefficient values are low for the random network, and those of the characteristic path length is high. A random network's null model is highly integrated and not segregated due to a lack locally of significant clustering between the nodes. These reference networks are used to calculate the ϕ of the observed network. EEG-based networks can show path lengths or clustering coefficients that exceed the lattice or random networks' length. If these weighted networks' measures are more significant than 1, they are assigned to 1, and if they are less than 0, they are set to 0, which guarantees that ϕ is limited in a range [0, 1].

The EEG-based networks with high characteristics of the small world (low ΔC and ΔL) will have ϕ close to 1, while lower values of ϕ are related to larger deviations from the corresponding zero models of clustering and path length, showing a smaller small-world structure and greatest characteristics of the small world. The network statistics ϕ, which accurately determine the small world's quantity in the network systems, is extremely sensitive to critical variables such as the strength of interconnections between nodes. The real power of ϕ is the ability to quantify the degree of small-world structure between different networks. The EEG networks show relatively large ϕ values, indicating that these networks as a whole do indeed exhibit the small-world properties. EEG networks with high small-world characteristics have a high value of ϕ (close to 1), driven by equally contributed high clustering and low path length (low ΔC and low ΔL). The relative high ϕ can also be driven by high clustering and moderate path length (low ΔC and moderate ΔL), as well as moderate clustering and low path length (moderate ΔC and low ΔL). While lower values of ϕ (less small-world structure) represent larger deviations from the respective null models for clustering and path length (Muldoon et al., 2016).

Here, the 40 by 40-weighted adjacency matrices were calculated separately in the frequency bands from δ to γ. The ϕ, ΔL, ΔC were calculated for dyslexics and controls, using the Brain Connectivity Toolbox for MATLAB, at http://www.seas.upenn.edu/~dsb/ (Muldoon et al., 2016). The ϕ, ΔL, ΔC were averaged between trials for each child in every frequency band and condition.

2.6.2 Local measures of functional connectivity hubs

The strengths and betweenness centrality (Bullmore and Sporns, 2009; Rubinov and Sporns, 2010; Stam and van Straaten, 2012) are local nodes' measures in the network topology. The betweenness centrality of the nodes is determined by converting the weights of the adjacency matrix into distances, i.e., larger correlations lead to smaller distances. The betweenness centrality of a node is the fraction of all shortest paths in the network that pass through a given node. The betweenness centrality of the edges is the fraction of all shortest paths in the network that contain a given edge. Edges with high values of betweenness centrality participate in a large number of shortest paths. The strength is the sum of all weights of connections for a given node. The values of the strength or BC of the nodes are normalized towards the average strengths or BCs across all network nodes. The nodes with high strength or BC participate in many shortest paths and play an important role in processing information in the graph (Boccaletti et al., 2006). The most important nodes of the network are the hubs. A graph with higher maximum strength or BC is assumed to be more integrated (Bullmore and Sporns, 2009; Stam and van Straaten, 2012). The hubs are defined as nodes with strength/or BC, averaged for each participant, at least one standard deviation above the mean group strength/or BC. The most important links are the maximal BC edges, averaged for each participant, representing at least one standard deviation above the mean group edge BC. The measures (e.g., strength, node BC, edge BC) were obtained via Matlab's brain connectivity toolbox (Rubinov and Sporns, 2010). The figures were generated using BrainNet Viewer version 1.63 (Xia et al., 2013).

2.7 Statistical analysis

In EEG recording sessions, the reaction times and performance accuracy of pre- and post-training dyslexic groups were compared for each condition (words/pseudowords) and dyslexics and neurotypical readers by Kruskal-Wallis nonparametric test (KW test).

For each frequency band and condition (word or pseudoword), a between-group pair comparison of each global SWP measure was performed by a nonparametric bootstrap procedure with 1000 random permutations (Maris and Oostenveld, 2007; Mason and Newton, 1990). Three graph indices (ϕ, ΔL, ΔC) were compared between the groups in 21 (three indices x seven frequencies) independent permutation tests with correction for multiple comparisons. A Bonferroni correction to the significance level was applied separately for the global tests ($P = \alpha/3 = 0.017$). The nodes' local measures (strength, BC) were investigated to evaluate the brain regions' local corporation, using separate non-parametric permutation cluster-based statistics (Maris and Oostenveld, 2007). The cluster-based nonparametric tests depend on a threshold used to select the nodes that will subsequently be clustered. This analysis was performed for that maximum BC/or maximal strength cross the selective threshold criteria to define a hub (one standard deviation over the average group nodal BC/or strength). The localization procedure involved identifying clusters based on their cluster statistics. The critical value for the (max cluster) statistics was used to identify significant clusters while controlling the false alarm rate with correction for multiple comparisons, where multiple clusters exhibited a significant difference and quantified the effect by their ordered sequence. Their indices in the histograms are chosen so that their medians are sensitive to hemispheric differences. The selected threshold based on the data required Bonferroni correction of the significance level to control for multiple thresholds ($P = \alpha/2 = 0.025$). Non-parametric statistical tests were performed in MATLAB. All the p-values that showed significant results are presented in bold text. The same selection criteria were performed separately for the edge BC, and the links, cross the threshold were presented in the figures.

3. Results

3.1 Behavioral results

The results of the between-group comparisons (K-W test) of the behavioral measures (percentage of correct answers and reaction

Table 1. Nonparametric statistical comparison of the behavioral parameters.

	Controls	*Pre-training Dys*	*Post-training Dys*	*Con/Pre-training Dys*		*Con/Post-training Dys*		*Pre-training/Post-training Dys*	
				P	χ^2	*P*	χ^2	*P*	χ^2
1. word									
Success	94.66 ± 1.15	69.83 ± 2.75	78.6 ± 2.99	**9.51e-08**	28.5	**8.07e-06**	19.2	**0.03**	4.51
RT	1149.1 ± 13.28	1333.8 ± 18.52	1369.3 ± 19.82	**3.75e-15**	61.8	**1.25e-21**	91.2	0.08	2.87
2. pseudo-word									
Success	91.7 ± 1.52	55.58 ± 3.71	69.5 ± 5.04	**1.26e-08**	32.4	**0.0003**	13.05	**0.02**	5.29
RT	1313.4 ± 15.21	1543.3 ± 22.6	1537.8 ± 22.2	**9.31e-18**	73.7	**3.69e-21**	89.1	0.7	0.07

$^{***}P < 0.001$, $^{**}P < 0.01$, $^{*}P < 0.05$; χ^2, df = 43, Kruskal-Wallis, Con - control group, Dys - dyslexics, success rate % (mean ± s.e.), RT - reaction time in ms (mean ± s.e.).

time) are shown in Table 1. The dyslexic group (before training and after training) showed a lower success rate and slower reaction times compared to the controls in both conditions (words and pseudowords: $P < 0.0003$, $\chi^2 > 13.05$). After training the dyslexics showed an improvement in the percentage of correct answers ($P = 0.03$, $\chi^2 = 4.51$ for words; $P = 0.02$, $\chi^2 = 5.29$ for pseudowords), their reaction times, however, did not change significantly ($P = 0.08$, $\chi^2 = 2.87$ for words; $P = 0.8$, $\chi^2 = 0.07$ for pseudowords).

3.2 Global SWP measures

Significant differences in all global SWP measures were found between the controls and the pre-training dyslexic group, as well as between pre- and post-training dyslexic groups in the θ, α, β, and γ frequency bands for the words and in α, β, γ for the pseudowords. A tendency of a decrease of ϕ, driven by an increase of ΔC and a decrease of ΔL with the increase of the frequency was observed in the groups from θ to $\beta 2$ frequency range, while this trend reverses in $\gamma 2$ - ϕ and ΔL increase, and ΔC decreases for all groups.

The pre-training dyslexics, compared to other groups, had statistically higher ϕ and ΔL in θ, α, β and $\gamma 1$ bands for word discrimination ($P < 0.007$, $\chi^2 > 7.25$; Table 2, except for ϕ in θ than the pre-training group), while for pseudoword discrimination - in β and $\gamma 1$ ($P < 0.012$, $\chi^2 > 6.39$; Table 3). They had a statistically lower ΔC *vs* controls (θ - $\gamma 1$, Table 2; β - $\gamma 1$, Table 3: $P < 0.002$, $\chi^2 > 10.06$) and *vs* post-training group (θ - $\gamma 1$, Tables 2, 3: $P < 0.006$, $\chi^2 > 7.4$). However, statistically lower ΔL and higher ΔC were observed at $\gamma 2$ for the pre-training group comparing to the other groups ($P < 0.0087$, $\chi^2 > 6.87$, Table 2 and Table 3; except for ΔL at the post-training group, Table 2), as well as a lower ΔL for δ than the post-training dyslexics (Table 2). Compared to the controls, the post-training dyslexics had a statistically lower ΔC in δ, higher ΔL in $\gamma 1$ and lower ΔL in $\gamma 2$ bands for the word discrimination (ΔC: $P = 0.003$, $\chi^2 = 7.8$; ΔL: $P < 0.005$, $\chi^2 > 7.75$; Table 2), while in $\gamma 1$ for the pseudoword discrimination - statistically higher ϕ and lower ΔC ($P < 0.014$, > 6.01; Table 3).

The groups' graphs exhibit small-world properties. A relatively high small-world propensity ϕ at low and medium frequencies gradually passes into networks with relatively moderate small-world propensity ϕ at high frequencies. The network with a relatively high ϕ was driven by a low clustering and low path length (high ΔC and low ΔL) at θ-frequency. In contrast, the network with relatively moderate ϕ was driven by an equally contributed moderate clustering and path length (moderate ΔC and moderate ΔL) at $\gamma 2$ frequency. While the lower values of ϕ at β-frequencies represented larger deviations from the respective null models for clustering and path length, then the EEG-based functional networks are rewired, most expressed in the post-training group. The controls and the post-training dyslexic group in $\gamma 2$ had nodes with a middle-long path and moderate locally significant clustering between the nodes. Therefore, the integration and segregation are moderate for word/pseudoword conditions and more segregated in the pseudoword condition for controls. For post-training dyslexics in $\gamma 2$-band, compared to pre-training dyslexics, the EEG network structure with an equal contribution of ΔC and ΔL, and increasingly ϕ becomes more segregated and less integrated, guided by a large ΔC for the word/pseudoword conditions (Tables 2, 3), and by the significantly higher change in the path ΔL for the pseudoword discrimination.

3.3 Topological distribution of functional connectivity hubs

For discrimination of words, the between-group comparisons in the θ-frequency band showed a significant difference in the hub distributions, based on the strength of nodes, between controls and pre-training children with dyslexia ($P = 2.28e\text{-}05$, $\chi^2 = 17.94$), as well as between controls and post-training dyslexics ($P = 0.007$, $\chi^2 = 7.12$; Table S2). The statistical comparisons between controls and dyslexic groups revealed that the typical readers had more hubs in the left hemisphere, while the pre-training dyslexics - in the right hemisphere. However, the post-training dyslexics, compared to the controls, had more hubs in the brain's posterior part. For the normally reading children, the hubs were located at the bilateral medial frontal cortex (MFC: Fz covers BA8 - intermediate frontal, including frontal eye fields; Giacometti et al. (2014); Koessler et al. (2009)) and middle temporal gyri (MTG; TP7-8: BA21), as well as the left middle frontal gyrus (MFG; FC3: BA6 - premotor cortex and supplementary motor cortex) the right-hemispheric ITG (P8: BA37 - occipitotemporal gyrus) and superior occipital gyrus (SOG; PO4: BA19 - associative visual cortex; Fig. 2A). The hubs for pre-training dyslexics were in the right superior frontal cortex (SFC; AF4: BA9), the right middle frontal gyrus (MFG; F4: BA8 - intermediate frontal cortex), the right precentral gyrus (PRECG; C2: BA4 - primary motor cortex), the left postcentral gyrus (PSTCG; C3: BA123 - primary somatosensory cortex), and the left middle temporal gyrus (MTG; T7: BA21). The hubs for post-training dyslexics encompassed the bilateral MFC (Fz), the left-hemispheric MFG (F3), PSTCG (C3, BA123 - primary somatosensory cortex; C5: BA123, BA40 - supramarginal gyrus),

Table 2. Nonparametric statistical comparisons of graph SWP metrics ϕ, ΔC, ΔL (mean $\pm$ s.e.) of functional brain networks of control and dyslexic groups during word discrimination for Frequency: δ = 1.5 ÷ 4; θ = 4 ÷ 8; α = 8 ÷ 13; $\beta 1$ = 13 ÷ 20; $\beta 2$ = 20 ÷ 30; $\gamma 1$ = 30 ÷ 48; $\gamma 2$ = 52 ÷ 70 Hz.

	Control	Pre-training Dys	Post-training Dys	Con vs. Pre-training Dys		Con vs. Post-training Dys		Pre-training vs. Post-training Dys	
				P	χ^2	*P*	χ^2	*P*	χ^2
δ									
ϕ	0.631 ± 0.010	0.643 ± 0.011	0.645 ± 0.015	0.382	0.76	0.207	1.59	0.65	0.2
$\triangle C$	0.429 ± 0.018	0.389 ± 0.019	0.339 ± 0.026	0.189	1.72	**0.003**	8.72	0.09	2.8
$\triangle L$	0.234 ± 0.011	0.232 ± 0.014	0.282 ± 0.017	0.421	0.65	0.030	4.69	**0.005**	7.8
θ									
ϕ	0.528 ± 0.007	0.559 ± 0.008	0.534 ± 0.008	**0.007**	7.25	0.419	0.65	0.07	3.2
$\triangle C$	0.636 ± 0.013	0.566 ± 0.014	0.623 ± 0.014	**0.0003**	13.4	0.394	0.73	**0.006**	7.4
$\triangle L$	0.141 ± 0.006	0.186 ± 0.009	0.146 ± 0.007	**4.11e-05**	16.8	0.637	0.22	**0.0004**	12.6
α									
ϕ	0.503 ± 0.006	0.548 ± 0.007	0.495 ± 0.007	**2.64e-06**	22.1	0.494	0.47	**2.9e-07**	26.4
$\triangle C$	0.684 ± 0.009	0.600 ± 0.012	0.691 ± 0.011	**6.65e-07**	24.7	0.582	0.30	**1.8e-07**	27.2
$\triangle L$	0.119 ± 0.004	0.147 ± 0.006	0.119 ± 0.006	**0.001**	10.8	0.614	0.26	**0.0006**	11.6
β_1									
ϕ	0.475 ± 0.006	0.501 ± 0.006	0.456 ± 0.006	**0.001**	10.9	0.152	2.05	**5.2e-06**	20.8
$\triangle C$	0.729 ± 0.009	0.689 ± 0.009	0.753 ± 0.009	**0.001**	12.1	0.137	2.22	**1.6e-06**	23
$\triangle L$	0.086 ± 0.004	0.101 ± 0.005	0.076 ± 0.004	**0.001**	9.70	0.059	3.56	**2.9e-06**	21.9
β_2									
ϕ	0.459 ± 0.006	0.502 ± 0.006	0.465 ± 0.006	**5.91e-08**	29.4	0.447	0.58	**5.0e-06**	20.8
$\triangle C$	0.756 ± 0.009	0.688 ± 0.009	0.746 ± 0.010	**1.92e-08**	31.6	0.452	0.56	**1.8e-06**	22.8
$\triangle L$	0.073 ± 0.003	0.094 ± 0.005	0.075 ± 0.004	**0.001**	11.2	0.833	0.04	**0.0025**	9.1
γ_1									
ϕ	0.499 ± 0.006	0.535 ± 0.007	0.510 ± 0.007	**1.91e-05**	18.3	0.102	2.68	**0.007**	7.2
$\triangle C$	0.693 ± 0.010	0.619 ± 0.011	0.673 ± 0.011	**3.58e-07**	25.9	0.065	3.39	**0.001**	10.5
$\triangle L$	0.101 ± 0.003	0.141 ± 0.007	0.117 ± 0.005	**6.07e-08**	29.3	**0.005**	7.75	**0.007**	7.3
γ_2									
ϕ	0.502 ± 0.007	0.515 ± 0.008	0.516 ± 0.009	0.547	0.36	0.273	1.20	0.7	0.12
$\triangle C$	0.379 ± 0.014	0.471 ± 0.016	0.406 ± 0.017	**8.59e-06**	19.8	0.213	1.55	**0.005**	8.0
$\triangle L$	0.463 ± 0.015	0.356 ± 0.014	0.403 ± 0.017	**5.41e-07**	25.1	**0.005**	7.99	0.08	3.0

Nonparametric statistical comparisons of the global metrics (small-world propensity ϕ; clustering coefficient ΔC; characteristic path length ΔL) of the brain networks of controls, pre-training and post-training dyslexic groups during discrimination of words for frequency bands: δ = 1.5-4; θ = 4-8; α = 8-13; $\beta 1$ = 13-20; $\beta 2$ = 20-30; $\gamma 1$ = 30-48; $\gamma 2$ = 52-70 Hz.

inferior parietal lobe (IPL; CP3: BA40 - supramarginal gyrus), as well as the bilateral superior parietal gyrus (SPL; Pz: BA7) and the right ITG (P8).

In the θ-frequency band for discrimination of words, there was also a significant difference in the distribution of hubs, based on a local measure betweenness centrality BC, between the controls and pre-training dyslexics (P = 0.003, χ^2 = 9.03; Table S2). For the control group, the hubs were found at the bilateral MFC (Fz), anterior part of the bilateral inferior temporal gyrus (ITG; FT9-10: BA20 - inferior temporal gyrus, Koessler et al., 2009; BA38 - temporal pole, Giacometti et al., 2014), right inferior frontal gyrus (IFG; F8: BA45/47 - Broca's area, orbital frontal cortex), left MTG (TP7), left ITG (P7; Fig. 2B). For the pre-training dyslexic group, the hubs were in the left inferior frontal gyrus (IFG; F7: BA45/47 - Broca's area, orbital frontal cortex), right PSTCG (C2), left ITL (FT9), left MTG (T7), right middle occipital gyrus (MOG; PO8, O2: BA18; Fig. 2B). The differences in the two groups' networks were due to the controls having more hubs in the left hemisphere, whereas the pre-training dyslexics were with more hubs in the right hemisphere. The between-group comparison of the hub distribution (BC) between controls and post-training dyslexics showed no statistical difference (P = 0.396, χ^2 = 0.72). There was no statistical difference between the two dyslexic groups (P = 0.04, χ^2 = 4.4). After training, the hubs were observed in the bilateral anterior part of ITL (FT9-10), left MTG (T7), left PSTCG (C5), the bilateral superior parietal (SPL; Pz) and in a part of the cuneus of the occipital lobe (Oz: BA18).

The between-group comparisons of the hub distributions (BC) in the α-band revealed a statistically significant difference between controls and the pre-training dyslexics (P = 0.023, χ^2 = 5.15, Table S2), where the dyslexics were showing more hubs in the right hemisphere. For the controls, the hubs with the largest BC were located in the bilateral MFC (Fz), left ITL (FT9), left MTG (T7), left ITG (P7), PSTCG (C5), left superior occipital gyrus (SOG; PO3: BA19), right MOG (PO8, O2), cuneus (Oz) (Fig. 2C). For pre-training dyslexics, the hubs were in the right ITL (FT10), the

Table 3. Nonparametric statistical comparisons of graph SWP metrics ϕ, ΔC, ΔL (mean $\pm$ s.e.) of functional brain networks of control and dyslexic groups during *pseudoword discrimination* for Frequency: δ = 1.5 ÷ 4; θ = 4 ÷ 8; α = 8 ÷ 13; $\beta 1$ = 13 ÷ 20; $\beta 2$ = 20 ÷ 30; $\gamma 1$ = 30 ÷ 48; $\gamma 2$ = 52 ÷ 70 Hz.

	Control	Pre-training Dys	Post-training Dys	Con vs. Pre-training Dys		Con vs. Post-training Dys		Pre-training vs. Post-training Dys	
				P	$\chi 2$	*P*	$\chi 2$	*P*	$\chi 2$
δ									
ϕ	0.662 ± 0.009	0.636 ± 0.009	0.627 ± 0.015	0.047	3.95	0.073	3.22	0.79	0.07
$\triangle C$	0.338 ± 0.019	0.380 ± 0.019	0.395 ± 0.027	0.073	3.21	0.128	2.31	0.87	0.03
$\triangle L$	0.268 ± 0.010	0.263 ± 0.011	0.270 ± 0.017	0.610	0.26	0.563	0.33	0.87	0.03
θ									
ϕ	0.520 ± 0.007	0.521 ± 0.008	0.519 ± 0.008	0.997	1.30e-05	0.889	0.02	0.89	0.02
$\triangle C$	0.638 ± 0.013	0.631 ± 0.014	0.646 ± 0.013	0.847	0.04	0.951	0.003	0.79	0.06
$\triangle L$	0.156 ± 0.007	0.162 ± 0.009	0.149 ± 0.007	0.959	0.003	0.509	0.44	0.49	0.45
α									
ϕ	0.498 ± 0.007	0.518 ± 0.007	0.501 ± 0.007	0.035	4.46	0.655	0.2	0.11	2.5
$\triangle C$	0.692 ± 0.011	0.657 ± 0.012	0.691 ± 0.011	0.026	4.98	0.693	0.16	0.07	3.3
$\triangle L$	0.115 ± 0.004	0.124 ± 0.006	0.108 ± 0.004	0.495	0.47	0.313	1.02	0.09	2.7
β_1									
ϕ	0.466 ± 0.006	0.498 ± 0.007	0.466 ± 0.007	**0.001**	12.09	0.781	0.08	**0.0017**	9.8
$\triangle C$	0.741 ± 0.009	0.697 ± 0.011	0.745 ± 0.011	**0.001**	11.57	0.906	0.01	**0.0012**	10.5
$\triangle L$	0.083 ± 0.005	0.092 ± 0.004	0.074 ± 0.004	**0.012**	6.39	0.219	1.51	**0.0004**	12.4
β_2									
ϕ	0.459 ± 0.006	0.498 ± 0.007	0.458 ± 0.006	**3.1e-06**	21.75	0.946	0.005	**1.4e-05**	18.9
$\triangle C$	0.757 ± 0.008	0.699 ± 0.010	0.757 ± 0.010	**2.4e-06**	22.22	0.933	0.007	**1.5e-05**	18.7
$\triangle L$	0.069 ± 0.003	0.086 ± 0.004	0.074 ± 0.004	**0.001**	10.59	0.379	0.77	0.02	5.2
γ_1									
ϕ	0.488 ± 0.006	0.535 ± 0.007	0.505 ± 0.006	**3.4e-07**	25.99	**0.014**	6.01	**0.0035**	8.5
$\triangle C$	0.713 ± 0.009	0.619 ± 0.012	0.684 ± 0.009	**2.4e-09**	35.62	**0.013**	6.16	**0.00029**	13.1
$\triangle L$	0.095 ± 0.003	0.140 ± 0.008	0.103 ± 0.004	**1.1e-05**	19.26	0.358	0.84	**0.0014**	10.2
γ_2									
ϕ	0.500 ± 0.007	0.504 ± 0.009	0.502 ± 0.009	0.982	0.001	0.969	0.001	0.97	0.001
$\triangle C$	0.418 ± 0.014	0.487 ± 0.017	0.419 ± 0.018	**0.002**	10.06	0.964	0.002	**0.0048**	7.95
$\triangle L$	0.436 ± 0.015	0.352 ± 0.015	0.416 ± 0.018	**7.3e-05**	15.72	0.368	0.81	**0.0087**	6.87

Nonparametric statistical comparisons of the global metrics of the brain networks of controls, pre-training and post-training dyslexic groups during pseudoword discrimination.

right PRECG (C2), the right SOG (PO4), the bilateral MOG (PO7-O8), the cuneus (Oz) (Fig. 2C). After training, the hubs with the largest BC for the dyslexics were found in the left ITL (FT9), right PRECG (C2), SPL (Pz), right ITG (P8), right SOG (PO4), right MOG (PO8, O2). The KW tests did not show significant differences in the hub distributions between controls and post-training dyslexics (P = 0.124, χ^2 = 2.36). There wasn't a significant difference between the two dyslexic groups, either (P = 0.55, χ^2 = 0.34).

In the $\beta 1$-frequency band, the hub distributions based on the strength were differed between controls and pre-training dyslexic group for word discrimination (P = 0.018, χ^2 = 5.58; Table S2), because the hub distribution of the pre-training dyslexics was shifted more towards the right hemisphere than the controls. For the controls, the hubs were located in the bilateral PSTCG (C4, C5-6), right MFG (FC4), right SPL (CP2: BA5 - somatosensory association cortex, Giacometti et al., 2014), right MOG (PO4), whereas for the pre-training dyslexics, the main hubs were in the right superior frontal gyrus (SFG, AF4), bilateral PRECG (C1-2), bilateral MFG (FC3: BA6, F3-F4: BA8), right PSTCG (C6), right SPL (CP2). For the post-training dyslexic group, the main hubs were in the bilateral MFC (Fz), PRECG (Cz, C2: BA4), left PSTCG (C3), right SPL (CP2), left inferior parietal lobe (IPL; CP3: BA40 - supramarginal gyrus), bilateral SPL (Pz: BA7 - somatosensory association cortex), left SOG (PO3; Fig. 2D). The difference between the controls and the post-training dyslexic group was not significant (P = 0.407, χ^2 = 0.69) as well as between both dyslexic groups (P = 0.14, χ^2 = 2.1).

For the pseudoword condition in the θ-frequency range, the between-group comparisons of the hub distributions (strength) revealed significant differences between controls and pre-training dyslexics (P = 0.003, χ^2 = 8.61; Table S3), with controls having more hubs in the posterior part in the brain. The main hubs for the controls were found in the bilateral IPL (CP3-4: BA40), the right PRECG (C2), the right SPL (CP2), the right ITG (P8), the right SOG (PO4), the right MOG (PO8, O2; Fig. 3A). The main hubs of pre-training dyslexics were in the bilateral PRECG (Cz, C1), the bilateral IPL (CP3: BA40, P4: BA39 - angular gyrus), bilat-

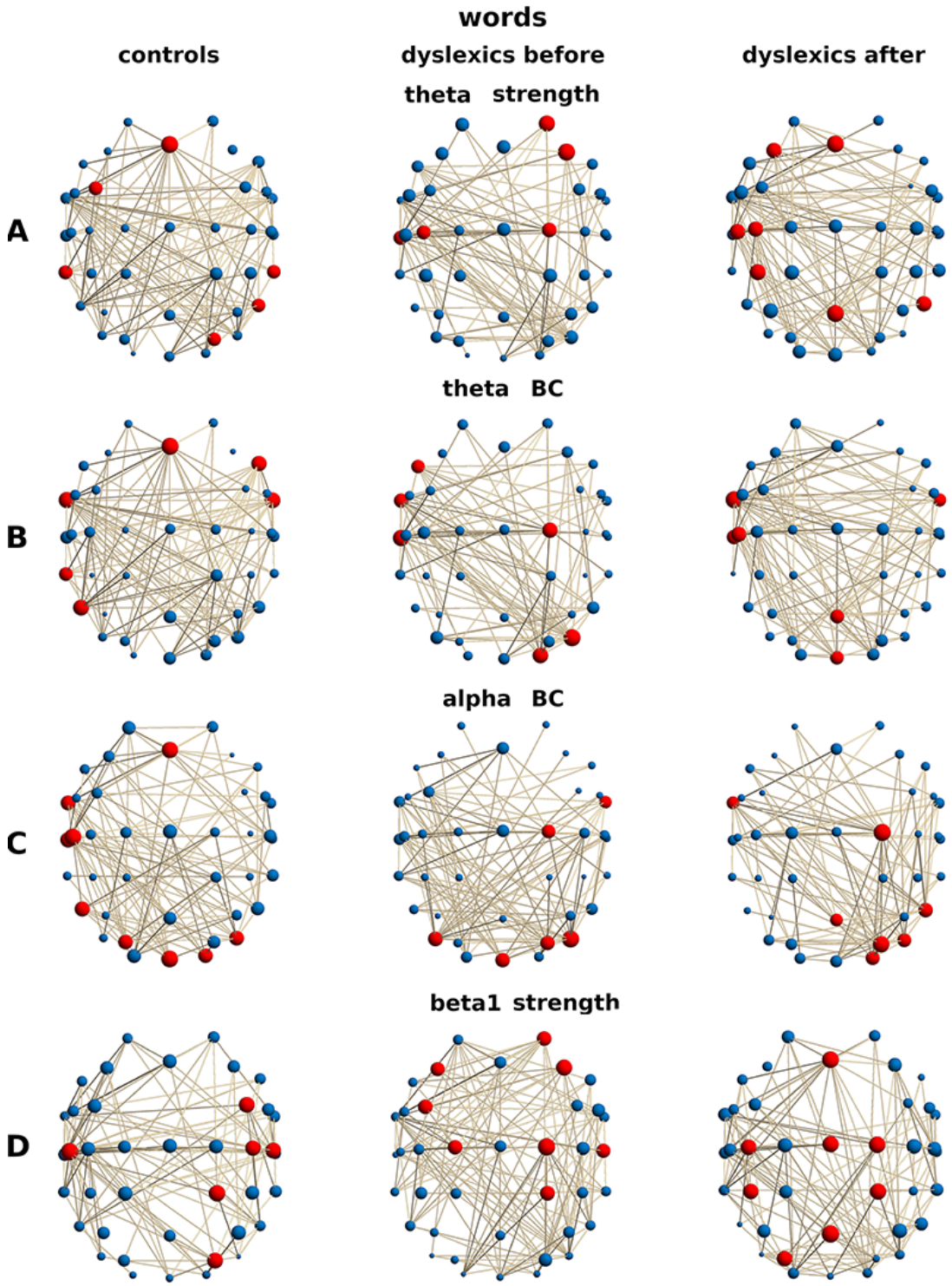

Fig. 2. The hubs on a group level for selected frequency bands for the word condition. Each node corresponds to an EEG sensor. The hubs, presented in red color, obtained from the group averaged strength/BC values. The links represent the most important links with edge BC: (**A, 1 graph**) Hubs (strength) in the θ-band for controls: Fz, FC3, TP7-8, P8, PO4; (**A, 2 graph**) for pre-training dyslexics: AF4, F4, C2, C3, T7; (**A, 3 graph**) for post-training dyslexics: Fz, F3, C3, C5, Pz, CP3, P8; (**B, 1 graph**) Hubs (BC) in the θ-band for the word condition for controls: Fz, FT9-10, F8, TP7, P7; (**B, 2 graph**) for pre-training dyslexics F7, FT9, T7, C2, PO8, O2; (**B, 3 graph**) for post-training dyslexics FT9-10, T7, C5, Pz, Oz. **(C, 1 graph**) Hubs (BC) in the α-band for controls: Fz, FT9, C5, T7, PO3, P7, PO8, O2, Oz; (**C, 2 graph**) for pre-training dyslexics FT10, C2, PO4, PO7-O8, Oz; (**C, 3 graph**) for post-training group FT9, C2, Pz, P8, PO4, PO8, O2. (**D, 1 graph**) Hubs (BC) in the β1-band for controls: FC4, C4, C5-6, CP2, PO4; (**D, 2 graph**) for pre-training dyslexics AF4, C1-2, FC3, F3-4, C6, CP2; (**D, 3 graph**) for post-training dyslexics Fz, Cz, C2, C3, CP2, CP3, Pz, PO3.

eral SPL (Pz), the left MOG (PO7). While for the post-training dyslexics, the main hubs were at bilateral MFC (Fz), the right inferior frontal gyrus (IFG; FC6: BA44/45 - opercular and triangular parts of Broca's area), the right PRECG (C2), the bilateral PSTCG (C3-4), the right SPL (CP2: BA5 - somatosensory association cortex), the right IPL (CP4) and the right MOG (PO4). Their significant differences in the hub distributions (P = 0.0127, χ^2 = 6.2) were due to the post-training group having more hubs in the brain's anterior part. However, there was no significant difference in hub distribution between controls and post-training dyslexic groups (P = 0.788, χ^2 = 0.07).

In the α-frequency range (pseudoword condition), the main hubs (strength) of the pre-training dyslexic group were in the left MFG (F3, FC3), the left IFG (FC5), the bilateral PSTCG (C3, C6), the left IPL (P3), the right MOG (O2; Fig. 3B). After training, they were located in the left MFG (F3), bilateral MFC (Fz), the left PSTCG (C5), the bilateral IPL (P3-4), the right SPL (CP2), the right MOG (PO4). There was a statistical difference between the hub distributions of the dyslexic groups (P = 0.011, χ^2 = 6.5, Table S3) due to more hubs in the anterior part of the left hemisphere of the post-training group. Controls' hubs were in the bilateral MFC (Fz), the bilateral PRECG (Cz), the left PSTCG (C3, C5), the bilateral SPL (Pz, CP2). In contrast, their distribution was not different from those of the dyslexic group before (P = 0.134) and after training (P = 0.264).

In the γ1-frequency range (pseudoword condition), the hub distributions of the controls and the pre-training dyslexics, based on the strength, were significantly different (P = 0.002, χ^2 = 9.97; Table S3), because the dyslexics had fewer hubs in the frontal cortex. The main hubs for the controls were observed in the right hemisphere at the superior frontal gyrus (SFG; AF4: BA9 - dorsolateral prefrontal cortex), MFG (F4), IFG (FC6), PSTCG (C4), SPL (CP2), IPL (CP4, P4), MOG (PO4; Fig. 3C). For the pre-training dyslexics, the hubs were in the right hemisphere at the MFG (FC4) IFG (FC6), PSTCG (C4, C6), SPL (CP2), IPL (CP4, P4), whereas after training, the hubs were in the right IFG (F8, FC6), PSTCG (C4, C6), MTG (T8), SPL (CP2), IPL (P4). The statistical tests didn't reveal any significant differences between the controls' hub distributions and the post-training dyslexic group (P = 0.774, χ^2 = 0.08). Compared to the pre-training dyslexic group, the post-training group's hub distribution contained more temporal hubs in the right hemisphere (P = 0.007, χ^2 = 7.2).

In the γ1-frequency range (pseudoword condition), the hub distributions (BC) of the control and the pre-training dyslexic groups were significantly different (P = 0.004, χ^2 = 8.21; Table S3) because the controls had more hubs in the left hemisphere. The hubs for the controls were located in the left ITL (FT9), the left MTG (T7), left PSTCG (C5), the right SPL (CP2) and the right MOG (PO4) (Fig. 3D), while for the pre-training dyslexics - in the right IFG (FC6), the right PSTCG (C6), the right ITL (FT10), the bilateral MTG (T7-8, TP8) and the left MOG (PO7; Fig. 3D). For the post-training dyslexics, the hubs were in the right IFG (FC6), the right PSTCG (C4), bilateral MTG (T7-8), the right SPL (CP2), the right IPL (P4), the right ITG (P8) and MOG (PO8). The statistical tests didn't reveal any significant differences between the hub distributions of controls and the post-training dyslexics (P = 0.374, χ^2 = 0.79), and between the dyslexic groups (P = 0.058, χ^2 = 3.6).

4. Discussion

4.1 Altered global topology in dyslexia

The groups show a small-world network structure in the functional connectivity, but with different characteristics. The networks in the groups exhibit properties that gradually change from higher small-world propensity, less local clustering and shorter path length (more integrated networks) at low frequencies (δ, θ, α; high ΔC and low ΔL) to lower small-word propensity, more moderate local clustering and moderate path length (γ2; close to more segregated networks) when the frequencies increase respectively from low and medium to high-frequency range. Networks with relative high small-world propensity ϕ at α-β frequencies pass towards networks with moderate ϕ at high γ2 frequency. Functional deficits in the weighted graphs were observed from θ to γ1-frequency bands in the dyslexics in the word/pseudoword discrimination task. The networks of the pre-training dyslexics compared to the typical readers and the post-training dyslexic group, had higher ϕ, driven by higher characteristics, which are more integrated and less segregated, and not well functionally specialized. The observed network variations in SWP characteristics are related to differences in the groups' task-specific brain network engagement. The network changes of controls and post-training groups in different frequencies would be associated with increased local network connectivity and decreased global integration.

In contrast, working memory load in pre-training dyslexics would be associated with decreased local network connectivity and increased global integration. The increased long-range connections integrating across distinct networks were observed in task-related α-frequency range (Vourkas et al., 2014). During a lexico-semantic task, the brain connectivity is different from connectivity patterns during rest or connectivity during passive observation of stimulus detection, which likely requires fewer brain networks (Krienen et al., 2014). Also, the segregation of two task-relevant networks, as a sensorimotor and a visual network, increases due to the training in the post-training group. Reduction in the involvement of other networks is in consequence of training. Increased network segregation during an automatic task could reflect the task-related network's greater autonomy and a less resource-intensive process (Bassett and Bullmore, 2017). The task, requiring motor execution, memory, and attention by engaged multiple brain networks, may temporarily induce long-range, integrative connections that are more unstable and costly metabolically than short, local connections (Cohen and D'Esposito, 2016). The balance of neural segregation (local efficiency) and integration (global efficiency, number of connector hubs) in the EEG network organization reflects the ability to adjust dynamically to current task demands. This balance contributes to the controls' successful task performance and the post-training dyslexics in a specific manner to the task's particular demands. Flexible network reconfiguration, balancing network segregation and integration, observed in the γ2 frequency band, may elucidate the optimal network structure underlying better performance of controls and post-training groups.

This finding is consistent with previous functional connectivity studies suggesting impaired network structure and mixed pat-

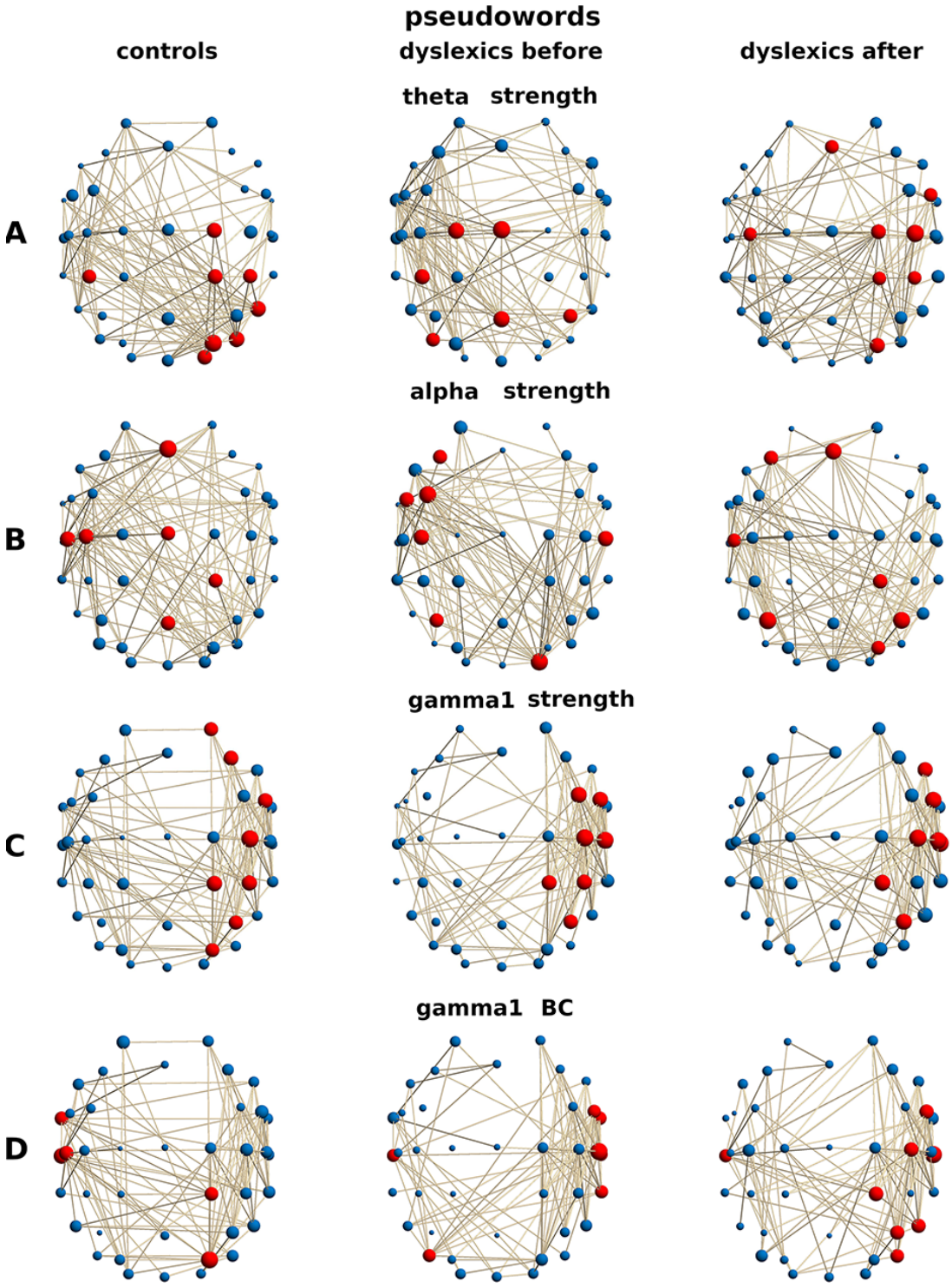

Fig. 3. The hubs on a group level for selected frequency bands for the pseudoword condition. (**A, 1 graph**) Hubs (strength) in the θ-band for controls: CP3-4, C2, CP2, P8, PO4, PO8, O2; (**A, 2 graph**) for pre-training dyslexics: C1, Cz, CP3, Pz, PO7; **(A, 3 graph**) for post-training dyslexics: Fz, C3-4, FC6, C2, CP2, CP4, PO4; (**B, 1 graph**) Hubs (strength) in the α-band for controls: F3, FC3, FC5, C3, C6, P3, O2; (**B, 2 graph**) for pre-training dyslexics F3, Fz, C5, P3-4, CP2, PO4; (**B, 3 graph**) for post-training dyslexics Fz, Cz, C3, C5, CP2, Pz. **(C, 1 graph**) Hubs (strength) in the γ1-band for controls: AF4, F4, FC6, C4, CP2, CP4, P4, PO4; (**C, 2 graph**) for pre-training dyslexics FC4, FC6, C4, C6, CP2, CP4, P4; (**C, 3 graph**) for post-training dyslexic group F8, FC6, C4, C6, T8, CP2, P4. (**D, 1 graph**) Hubs (BC) in the γ1-band for controls: FT9, C5, T7, CP2, PO4; (**D, 2 graph**) for pre-training dyslexics FC6, FT10, C6, T7-8, TP8, PO7; (**D, 3 graph**) for post-training dyslexics FC6, C4, T7-8, CP2, P4, P8, PO8.

terns of connectivity abnormalities in dyslexia (Frye et al., 2012; Koyama et al., 2013). The typical direction of the network development in children revealed an age-related decrease in brain specialization with a gradual strengthening of long-distance connections (Hagmann et al., 2010). The children's brain maturation has been associated with a global decrease of slow-wave activity, including theta oscillations, correlated with language abilities at all ages, and increased higher frequencies (Gaudet et al., 2020). The efficient network architecture optimally balances between local processing and global integration (Bullmore and Sporns, 2012) in the post-training group, most pronounced in $\gamma 2$ frequency. In comparison, the network for the pre-training group with dyslexia reflects a less optimal global organization even in $\gamma 2$ frequency. In higher frequency bands (β), a network with a more segregated and locally specialized, but a less integrated organization has a higher degree of information transfer between neighbor brain areas with less long-distance information exchange with increasing task demands (Vourkas et al., 2014). The reorganization networks found in post-training dyslexics may reflect compensatory mechanisms for the delayed and deferred establishment of the connections over long distances that stimulate the neuroplasticity, strengthen the EEG networks weakened by dyslexia, and correct this disorder (Ercsey-Ravasz et al., 2013; Finn et al., 2014; Magosso et al., 2017; Ursino et al., 2015).

Lower theta frequencies mediate the integration of long distances between processes involving several cortical regions (von Stein and Sarnthein, 2000). The θ frequencies are associated with long-distance interactions during top-down processes, such as working memory retention (von Stein and Sarnthein, 2000), executive functions such as problem-solving, planning, working memory, and attention (Mizuhara and Yamaguchi, 2007; Sauseng et al., 2005). The impaired functional segregation and integration in developmental dyslexia at the theta frequencies could be associated with the task-related attention deficit and the disruption of the working memory, self-control, and the speed of processing language comprehension dyslexics (Sauseng et al., 2007). The present study results support previous evidence suggesting abnormalities in theta oscillations associated with reading difficulties (Arns and Peters, 2007; Bastiaansen et al., 2008; Goswami, 2011; Klimesch, 1999; Spironelli et al., 2008). The significant differences between pre-training dyslexics and the other groups in a wide α-frequency range were the lower and upper-frequency alpha bands' involvement in various cognitive and verbal memory processes (van Diessen et al., 2015). In the β-frequency band, the EEG network metric differences between the groups relate to the phonological decoding ability, top-down in syntactic and semantic mechanisms in the word/pseudoword reading (Gaudet et al., 2020; Vourkas et al., 2011). The global organization of functional brain networks was compromised in dyslexics. At low and middle EEG frequencies, less efficient long-distance connections in the networks of people with dyslexia, suggesting impaired functional connectivity between remote cortical areas of the reading network (Sandak et al., 2004), and also functional connectivity disorders in multiple brain networks outside the dyslexic reading network (Finn et al., 2014). The specific role of the γ-band in the phonological perception and assessment of the contextual lexico-semantic correspondence of incoming words/pseudowords could explain the different stages of the network metrics during typical brain maturation (Gaudet et al., 2020). The global measures characterized the change of the functional connectivity after intervention visual training, from which the subsequent widespread topological differences in the functional connectivity of dyslexics would be compatible with theoretical approaches suggesting a deficit in general sensory and attention functions.

Increasing topological segregation is associated with increased functional specialization of most brain areas that become less central in the network. The global change between the group comparisons increases in the frequency ranges: θ - $\gamma 1$ for words and $\beta 1$ - $\gamma 1$ for pseudoword condition, as well as the network constraints occurring in different physiological architectures. The age reorganization in children with developmental dyslexia, becoming segregated during childhood, is characterized by a shift of the EEG network topology from a centralized configuration to a decentralized one during the development.

4.2 Topological changes of hub regions

The analysis of the BC and strength of the nodes show theta associated regional abnormality in developmental dyslexia, which may suggest that the attention deficit in developmental dyslexia is linked not only to the whole brain's functional connectivity but with those in specific nodes. During the word condition in controls and post-training dyslexic groups, bihemispheric hubs were observed in the medial frontal cortex (θ_{str}, α_{BC}), anterior and middle temporal (θ_{str}), superior parietal ($\theta_{str,BC}$, α_{BC}, $\beta 1_{str}$), and middle occipital gyri (α_{BC}), which were absent in both hemispheres or very rarely present in one hemisphere of the pre-training children with developmental dyslexia. Theta oscillations being linked to lexical retrieval operations and semantic working memory, while alpha being linked to task-specific working memory load (Bastiaansen et al., 2005; Meyer et al., 2013; Weiss et al., 2005), and beta oscillations reflect syntactic unification operations (Lewis et al., 2015). The alpha coupling modulations with the theta in temporal and frontal areas and low beta-frequencies in parietal areas are associated with synchrony between distant inter-regional neural populations in both hemispheres, which are involved in the stimuli processing (Lewis and Bastiaansen, 2015). The left temporal cortical areas are responsible for retrieving lexical structure's memory to form a meaningful interpretation, containing phonological, syntactic, and semantic properties of individual words (Lewis and Bastiaansen, 2015). The functional connections of the middle temporal gyri have a crucial role in language comprehension at the level of single words. More anterior temporal areas are associated with conceptual object representations (Rice et al., 2015). Frontal regions are engaged in unification operations (Hagoort, 2013), integrating lexical units into a larger context. The middle temporal gyri's functional connections to more anterior temporal and frontal areas support the information propagation about individual lexical items to areas that subserve integration operations. These results could be explained with feedforward connections, functionally characterized by θ-frequency synchronization, and feedback connections by α and β frequency synchronization in the visual system (Michalareas et al., 2016). The remediation status affects the dysfunction of the dorsal (occipitoparietal sublexical, α_{BC}) route in developmental dyslexia and facilitates signal propagation to the weakly connected

bihemispheric frontal areas (α_{BC}). The feedback projections remove from the large-scale network while maintaining stability for the more strongly connected core areas in the right hemispheric ventral route (α_{BC}). As well as main hubs in occipitotemporal ($\theta_{st,BC}$, α_{BC}) and superior occipital gyri (θ_{st}, $\beta 1_{str}$) were also not presented in the pre-training dyslexics. Regarding the group without training, the controls showed more hubs of functional connectivity in the left fusiform/superior occipital gyri, while the trained group with dyslexia - in the right fusiform/superior occipital gyri (α_{BC}), as well as in the middle frontal cortex and the left superior occipital gyrus ($\beta 1_{str}$). In controls, beta oscillations predominate in the local occipital cortex or the frontal cortex and the left angular gyrus, maintaining the propagation of top-down information, processed in the EEG networks for the memory lexical retrieval, to lower levels in the cortical hierarchy (Bressler and Richter, 2015). A reduction of beta oscillations in these regions in non-trained dyslexics is associated with a change in the cognitive networks (the cognitive loop to achieve specific goals) due to suppressing the top-down information flow to revise the current meaning representation (Bressler and Richter, 2015). These results suggest that behavioral remediation may be associated with compensatory changes in the base of an atypically stronger connection between the posterior areas (superior occipital gyrus, fusiform gyrus, and left superior parietal lobe ($\alpha_{BC,}$ $\beta 1_{str}$) during word discrimination. Therefore, the feedforward and feedback connections are likely to be more distinct in peripheral sensory systems than in higher cortical regions (Ercsey-Ravasz et al., 2013; Finn et al., 2014). However, during visual discrimination of pseudowords, this remediation at α_{str} may be associated with compensatory changes based on greater functional connectivity between the right middle occipital gyrus and the bihemispheric middle frontal cortex as well as bihemispheric angular gyrus. The absence of lexical structure strengthens the need for information transfer to the "high-order" regions, possibly facilitating word meaning. The generation of a word form percept might require stronger interactions for effective processing in the absence of the context-constrained lexical structure. The specific carrier frequency in the network that supports the feedforward and feedback communications between parietal and frontal areas deviates from the observed network in the controls' visual system.

The processes of the font-perception in the right hemisphere (θ_{str}, $\gamma 1_{str}$) and an implicit lips-reading in the left hemisphere (θ_{str}, $\gamma 1_{BC}$), observed in the pseudoword condition, coexist with processes involved in the bihemispheric presentation of single words and faces (Behrmann and Plaut, 2020). In the pseudoword discrimination at θ_{st} frequencies, the right inferior and bilateral middle frontal regions are more likely to participate in earlier stages of font-perception learning of the post-training dyslexics. In contrast, bilateral primary motor cortices in the pre-training dyslexics are more involved in the silent lips-reading. In the controls, these connections expand from the bihemispheric supramarginal gyri and the superior parietal lobe to the right inferior temporal lobe, which are more likely to participate in the syllabic processing for θstr and constitutes one of the fundamental stages of bottom-up language processing.

The hubs in the right orbitofrontal cortex, the Broca's area, and the right middle temporal cortex are more likely to participate in earlier stages of learning in the post-training dyslexics in $\gamma 1_{str}$ frequencies, associated with phonological perception and assessment of the contextual lexical fit of incoming pseudowords, regions not observed in the pre-training dyslexic group. In $\gamma 1_{BC,}$ these functional connections ramify to the right and left temporal lobes, right superior and inferior parietal gyri, and the right inferior temporal lobe only in the post-training dyslexics, not in the pre-training group. For controls at $\gamma 1_{BC}$, this network also encompasses the left hemisphere ramifying to the middle part of the left temporal, inferior temporal gyri and the left angular gyrus, transferring further to the left anterior temporal lobe. The gamma oscillatory is linked to unification operations in lexico-semantic functions and the maintenance/change of the current cognitive set (Lewis et al., 2015). Gamma oscillations might promote bottom-up interactions during the occipital cortex processing and between the left inferior frontal cortex and left middle temporal cortex (Bastos et al., 2012) and provide bottom-up information over faster time scales in post-training dyslexics (Finn et al., 2014).

The frontal cortex and anterior temporal lobes (ATLs), the supramarginal and angular gyri (SMG, AG) as well as the right occipital lobe as incoming information area are assumed to involve in the lexico-semantic processing as nodes of the functional connectivity in the EEG network during the word/pseudoword visual discrimination. Besides these nodes, the modality-specific semantic access in the sensorimotor cortex was observed in the controls and the post-training dyslexics in $\beta 1_{str,(word)}$ and $\alpha_{str,\ (pseudoword)}$ frequency activity associated with syntactic and semantic binding mechanisms in the language processing, which could explain their faster performance compared to the pre-training dyslexic group. Unlike the pre-training dyslexics having a hub in one hemispheric ATL, the greatest effects of information transfer were observed between the two anterior temporal lobes in controls and dyslexics after training, as the bihemispheric ATLs which, among others are involved in semantic processing of words at θ_{BC} frequencies.

In children with dyslexia, before training, the nodes in the right ATL are observed together with nodes in the right somatosensory cortex in $\beta 1_{BC}$ for word condition, while nodes in the right ATL are observed together with nodes in the right orbitofrontal cortex for pseudoword condition in $\gamma 1_{BC}$. In the controls, the observed nodes in the left ATL were observed together with the left supramarginal gyrus for word (α_{BC}) and pseudoword discrimination ($\gamma 1_{BC}$). After training, in the children with developmental dyslexia, the nodes were observed in the left supramarginal gyrus and the bilateral middle frontal gyrus in $\beta 1_{str,\ word}$ and $\alpha_{BC,\ pseudoword}$. We assume that the heteromodal semantic subnet is coordinated by a node that connects the input somatosensory areas to the rest of the semantic network. The hub is dynamically shifted from ATL to SMG/AG from the left hemisphere in the controls to the right hemisphere in developmental dyslexia. The training in the visual modality also affects the distribution of nodes in children with developmental dyslexia. Therefore, the research confirms the hypothesis that the disturbed phonological decoding in dyslexia, occurring in the processing of visual and auditory dynamic stimuli, is influenced positively after training in the visual modality (Harrar et al., 2014; Lallier et al., 2010). The use of a task-solving paradigm for visual word recognition, which is commonly used in previous studies of fMRI (Binder et al., 2005) and

the EEG/MEG (Dhond et al., 2007) presumes that heteromodal, as well as some modality-specific areas, are involved in the semantic processing. The study of functional connectivity reveals cortical markers of dyslexia with promising prospects for monitoring neuronal changes associated with behavioral improvement (remediation).

For the controls and post-training dyslexics, the appearance of nodes simultaneously in the left-hemispheric medial frontal, occipitotemporal, anterior and middle temporal gyri at $\alpha_{BC,\ word}$, as well as the superior parietal, anterior and middle temporal gyri at $\gamma 1_{BC,\ pseudoword}$, the bihemispheric middle frontal and inferior parietal lobes at $\alpha_{str,\ pseudoword}$, is not observed in pre-training dyslexics. That suggests the continued development of the relationships between these regions. The presence of cortical nodes in children with developmental dyslexia after training in the dorsal visual network, mainly in the left hemisphere, suggests an effect of training on reading skills achievement. Brain areas become less central and more specialized locally, with network segregation during development balancing the benefits of integration between distant brain regions to the risks of congestion in central areas.

4.3 Conclusions

The "reading network", activating during reading, includes the "visual word form area" in the extrastriate cortex, the somatosensory association cortex, the superior and inferior parietal cortices, premotor and motor cortices (Taskov and Dushanova, 2020). These regions are a part of other networks, particularly those of the dorsal attention system. Reading is an important process, spending a lot of time exercising. The regions, incorporated with the reading task, are also utilized for the lexico-semantic network. The specific reading links may not represent routine functional relationships of many of the involved regions in dyslexia. Behavioral flexibility may depend on the ability to usefully configure the network of regions for specific tasks. These configurations are not necessarily representative of the basic way in which these regions are "normally" conjoined. Reading in dyslexia involves disrupting the baseline network's coherence to create task-specific new networks bound by new sets of dynamic relationships. These relationships render brain networks capable of flexible, adaptive response when the cognitive network maintains recognizable topology across individuals and retains additional freedom for context, stimulus, and task-dependent reconfiguration. Different networks have different contributions. Some may be more engaged in specific processes (visual, motor, reading). Others may be more important for integrating multimodal information or for task switching and control. Together with changes in the properties of the semantic network and the distribution of nodes, the results reveal that the analysis of functional networks can be a promising tool for reflecting the neuropathological mechanism of developmental dyslexia. This network task-specific view provides a basis for understanding the underlying of the reading network in dyslexia.

Author contributions

JD and ST conceived and designed the experiments; JD performed the experiments; JD and ST analyzed the data; JD wrote the paper; ST revised the paper.

Ethics approval and consent to participate

The Institute of Neurobiology, BAS, approved the research. Informed consent was obtained.

Acknowledgment

The study was supported by SNF DN05/14-2016. The authors would like to express their gratitude to the psychologist Dr. Y. Lalova and the logopedist A. Kalonkina for administering and scoring the psychological tests. A grant from the National Science Fund of the Ministry of Education and Science (project DN05/14-2016).

Conflict of Interest

The authors declare no conflict of interest.

Supplementary material

Supplementary material associated with this article can be found, in the online version, at https://jin.imrpress.com/EN/10.31083/j.jin.2020.04.193.

Submitted: June 16, 2020
Revised: November 07, 2020
Accepted: November 12, 2020
Published: December 30, 2020

References

Annett, M. (1970) A classification of hand preference by association analysis. *British Journal of Psychology* **61**, 303-321.

Arns, M. and Peters, S. (2007) Different brain activation patterns in dyslexic children: Evidence from EEG power and coherence patterns for the double-deficit theory of dyslexia. *Journal of Integrative Neuroscience* **6**, 175-190.

Bassett, D. S. and Bullmore, E. T. (2017) Small-world brain networks revisited. *The Neuroscientist* **23**, 499-516.

Bassett, D. S., Nelson, B. G., Mueller, B. A., Camchong, J. and Lim, K. O. (2012) Altered resting state complexity in schizophrenia. *NeuroImage* **59**, 2196-2207.

Bastiaansen, M. C. M., Oostenveld, R., Jensen, O. and Hagoort, P. (2008) I see what you mean: Theta power increases are involved in the retrieval of lexical semantic information. *Brain and Language* **106**, 15-28.

Bastiaansen, M. C. M., van der Linden, M., Keurs, M. T., Dijkstra, T. and Hagoort, P. (2005) Theta responses are involved in lexical-semantic retrieval during language processing. *Journal of Cognitive Neuroscience* **17**, 530-541.

Bastos, A. M., Usrey, W. M., Adams, R. A., Mangun, G. R., Fries, P. and Friston, K. J. (2012) Canonical microcircuits for predictive coding. *Neuron* **76**, 695-711.

Behrmann, M. and Plaut, D. C. (2020) Hemispheric organization for visual object recognition: A theoretical account and empirical evidence. *Perception* **49,** 373-404.

Benassi, M., Simonelli, L., Giovagnoli, S. and Bolzani, R. (2010) Coherence motion perception in developmental dyslexia: A meta-analysis of behavioral studies. *Dyslexia* **16**, 341-357.

Binder, J. R., Desai, R. H., Graves, W. W. and Conant, L. L. (2009) Where is the semantic system? A critical review and meta-analysis of 120 functional neuroimaging studies. *Cerebral Cortex* **19**, 2767-2796.

Binder, J. R., Westbury, C. F., McKiernan, K. A., Possing, E. T. and Medler, D. A. (2005) Distinct brain systems for processing concrete and abstract concepts. *Journal of Cognitive Neuroscience* **17**, 905-917.

Boccaletti, S., Latora, V., Moreno, Y., Chavez, M and Hwanga, D. U. (2006) Complex networks: Structure structure and dynamics. *Physics Reports* **424**, 175-308.

Boets, B., Vandermosten, M., Cornelissen, P., Wouters, J. and Ghesquière, P. (2011) Coherent motion sensitivity and reading development in the

transition from prereading to reading stage. *Child Development* **82**, 854-869.
Bressler, S. L. and Richter, C. G. (2015) Interareal oscillatory synchronization in top-down neocortical processing. *Current Opinion in Neurobiology* **31**, 62-66.
Bullmore, E. and Sporns, O. (2009) Complex brain networks: Graph theoretical analysis of structural and functional systems. *Nature Reviews Neuroscience* **10**, 186-198.
Bullmore, E. and Sporns, O. (2012) The economy of brain network organization. *Nature Reviews Neuroscience* **13**, 336-349.
Castles, A. and Coltheart, M. (1993) Varieties of developmental dyslexia. *Cognition* **47**, 149-180.
Chouake, T., Levy, T., Javitt, D. C. and Lavidor, M. (2012) Magnocellular training improves visual word recognition. *Frontiers in Human Neuroscience* **6**, 14.
Cohen, J. R. and D'Esposito, M. (2016) The segregation and integration of distinct brain networks and their relationship to cognition. *The Journal of Neuroscience* **36**, 12083-12094.
Coltheart, M., Rastle, K., Perry, C., Langdon, R. and Ziegler, J. (2001) DRC: A dual route cascaded model of visual word recognition and reading aloud. *Psychological Review* **108**, 204-256.
Cornelissen, P. L., Hansen, P. C., Hutton, J. L., Evangelinou, V. and Stein, J. F. (1998) Magnocellular visual function and children's single word reading. *Vision Research* **38**, 471-482.
Cuppini,C., Ursino, M., Magosso, E., Ross, L. A., Foxe,J. J. and Molholm, S. (2017) A computational analysis of neural mechanisms underlying the maturation of multisensory speech integration in neurotypical children and those on the autism spectrum. *Frontiers in Human Neuroscience* **11**, 518.
Dekker, T. M., Ban, H., van der Velde, B., Sereno, M. I., Welchman, A. E. and Nardini, M. (2015) Late development of cue integration is linked to sensory fusion in cortex. *Current Biology* **25**, 2856-2861.
Demb, J. B., Boynton, G. M., Best, M. and Heeger, D. J. (1998) Psychophysical evidence for a magnocellular pathway deficit in dyslexia. *Vision Research* **38,**1555-1559.
Dhond, R. P., Witzel, T., Dale, A. M. and Halgren, E. (2007) Spatiotemporal cortical dynamics underlying abstract and concrete word reading. *Human Brain Mapping* **28**, 355-362.
Dushanova, J. and Christov M. (2013) Auditory event-related brain potentials for an early discrimination between normal and pathological brain aging. *Neural Regeneration Research* **8**, 1390-1399.
Ebrahimi, L., Pouretemad, H., Khatibi, A. and Stein, J. (2019) Magnocellular based visual motion training improves reading in Persian. *Scientific Report* **9,** 1142.
Eden, G. F., VanMeter, J. W., Rumsey, J. M., Maisog, J. M., Woods, R. P. and Zeffiro, T. A. (1996) Abnormal processing of visual motion in dyslexia revealed by functional brain imaging. *Nature* **382**, 66-69.
Ercsey-Ravasz, M., Markov, N. T., Lamy, C., Van Essen, D. C., Knoblauch, K., Toroczkai, Z. and Kennedy, H. (2013) A predictive network model of cerebral cortical connectivity based on a distance rule. *Neuron* **80**, 184-197.
Facoetti, A., Lorusso M. L., Paganoni P., Umiltà C. and Mascetti, G. G. (2003) The role of visuospatial attention in developmental dyslexia: Evidence from a rehabilitation study. *Cognitive Brain Research* **15**, 154-164.
Farahibozorg, S., Henson, R. N., Woollams, A. M. and Hauk, O. (2019) 'Distinct roles for the anterior temporal lobe and angular gyrus in the spatio-temporal cortical semantic network'. *bioRxiv* doi: https://doi.org/10.1101/544114.
Finn, E. S., Shen, X., Holahan, J. M., Scheinost, D., Lacadie, C., Papademetris, X., S. E. Shaywitz, Shaywitz B. A. and Constable R. T. (2014) Disruption of functional networks in dyslexia: A whole-brain, data-driven analysis of connectivity. *Biological Psychiatry* **76**, 397-404.
Frye, R. E., Liederman, J., Fisher, J. M. and Wu, M. H. (2012) Laterality of temporoparietal causal connectivity during the prestimulus period correlates with phonological decoding task performance in dyslexic and typical readers. *Cerebral Cortex* **22,** 1923-1934.
Funnell, E. (1983) Phonological processes in reading: New evidence from acquired dyslexia. *British Journal of Clinical Psychology* **74**, 159-180.
Gaudet, I., Hüsser, A., Vannasing, P. and Gallagher, A. (2020) Functional brain connectivity of language functions in children revealed by EEG and MEG: A systematic review. *Frontiers in Human Neuroscience* **14**, 62.
Giacometti, P., Perdue, K. L. and Diamond, S. G. (2014) Algorithm to find high density EEG scalp coordinates and analysis of their correspondence to structural and functional regions of the brain. *Journal of Neuroscience Methods* **229**, 84-96.
Girolami-Boulinier, A. (1985) *Contrôle des Aptitudes à la Lecture et à l'Ecriture (CALE)*. Paris, Masson. (In French)
Goodale, M. A. and Westwood, D. A. (2004) An evolving view of duplex vision: separate but interacting cortical pathways for perception and action. *Current Opinion in Neurobiology* **14**, 203-211.
Goswami, U. (2011) A temporal sampling framework for developmental dyslexia. *Trends in Cognitive Sciences* **15**, 3-10.
Hagmann, P., Sporns, O., Madan, N., Cammoun, L., Pienaar, R., Wedeen, V. J., Meuli, R., Thiran, J. P. and Grant, P. E. (2010) White matter maturation reshapes structural connectivity in the late developing human brain. *Proceedings of the National Academy of Sciences of the United States of America* **107**, 19067-19072.
Hagoort, P. (2013) MUC (Memory, Unification, Control) and beyond. *Frontiers in Psychology* **4**, 416.
Harrar, V., Tammam, J., Pérez-Bellido, A., Pitt, A., Stein, J. and Spence, C. (2014) Multisensory integration and attention in developmental dyslexia. *Current Biology* **24**, 531-535.
Hodges, J. R. and Patterson, K. (2007) Semantic dementia: A unique clinicopathological syndrome. *The Lancet Neurology* **6,**1004-1014.
Jobard,G., Crivello, F. and Tzourio-Mazoyer, N. (2003) Evaluation of the dual route theory of reading: A meta-analysis of 35 neuroimaging studies. *Neuroimage* **20**, 693-712.
Joshi, M. R. and Falkenberg, H. K. (2015) Development of radial optic flow pattern sensitivity at different speeds. *Vision Research* **110**, 68-75.
Kalonkina, A. and Lalova, Y. (2016) Normative indicators for the test battery for a written speech assessment. In, Tyubele, S. and Iossifova, R. (eds.) *Logopedical Diagnostics (pp. 30-38).* Bulgaria: Rommel Publishing House.
Klimesch, W. (1999) EEG alpha and theta oscillations reflect cognitive and memory performance. A review and analysis. *Brain Research Reviews* **29**, 169-195.
Koessler, L., Maillard, L., Benhadid, A., Vignal, J. P., Felblinger, J., Vespignani, H. and Braun, M. (2009) Automated cortical projection of EEG sensors: Anatomical correlation via the international 10-10 system. *NeuroImage* **46**, 64-72.
Koyama, M. S., Di Martino, A., Kelly, C., Jutagir, D. R., Sunshine, J., Schwartz, S. J., Castellanos, F. X. and Milham, M. P. (2013) Cortical signatures of dyslexia and remediation: An intrinsic functional connectivity approach. *PLoS One* **8**, e55454.
Kravitz, D. J., Saleem, K. S., Baker, C. I. and Mishkin, M. (2011) A new neural framework for visuospatial processing. *Nature Reviews Neuroscience* **12**, 217-230.
Krienen, F., Yeo, T. and Buckner, R. (2014) Reconfigurable task-dependent functional coupling modes cluster around a core functional architecture. *Philosophical Transactions of the Royal Society B: Biological Sciences* **369**, 20130526.
Lallier, M., Tainturier, M. J., Dering, B., Donnadieu, S., Valdois, S. and Thierry, G. (2010) Behavioral and ERP evidence for amodal sluggish attentional shifting in developmental dyslexia. *Neuropsychologia* **48**, 4125-4135.
Lalova, J., Dushanova, J., Kalonkina, A. and Tsokov, S. (2019) Application of specialised psychometric tests and training practices in children with developmental dyslexia. *Psychological Research* **22**, 271-283.
Lalova, J., Dushanova, J., Kalonkina, A., Tsokov, S., Hristov, I., Totev, T. and Stefanova, M. (2018) Vision and visual attention of children with developmental dyslexia. *Psychological Research* **21**, 247-261.
Lawton, T. (2011) Improving magnocellular function in the dorsal stream remediates reading deficits. *Optometry & Vision Development (OVD) Journal* **42**, 142-154.

Lawton, T. (2016) Improving dorsal stream function in dyslexics by training figure/ground motion discrimination improves attention, reading fluency, and working memory. *Frontiers in Human Neuroscience* **10**, 397.

Lawton, T. and Shelley-Tremblay, J. (2017) Training on movement figure-ground discrimination remediates low-level visual timing deficits in the dorsal stream, improving high-level cognitive functioning, including attention, reading fluency, and working memory. *Frontiers in Human Neuroscience* **11**, 236.

Lewis, A. G. and Bastiaansen, M. (2015) A predictive coding framework for rapid neural dynamics during sentence-level language comprehension. *Cortex* **68**, 155-168.

Lewis, A. G., Wang, L. and Bastiaansen, M. C. M. (2015) Fast oscillatory dynamics during language comprehension: Unification versus maintenance and prediction? *Brain and Language* **148**, 51-63.

Liao, L. D., Wang, I. J., Chen, S. F., Chang, J. Y. and Lin, C. T. (2011) Design, fabrication and experimental validation of a novel dry-contact sensor for measuring electroencephalography signals without skin preparation. *Sensors* **11**, 5819-5834.

Magosso, E., Cuppini, C. and Bertini, C. (2017) Audiovisual rehabilitation in hemianopia: A model-based theoretical investigation. *Frontiers in Computational Neuroscience* **11**, 113.

Maris, E., and Oostenveld, R. (2007) Nonparametric statistical testing of EEG-and MEG-data. *Journal of Neuroscience Methods* **164**, 177-190.

Mason, M. and Newton, M. (1990) A rank statistics approach to the consistency of the general bootstrap. *The Annals of Statistics* **20,** 1611-1624.

Matanova, V. and Todorova, E. (2013) DDE-2 Testova bateriya za otsenka na disleksiya na razvitieto - balgarska adaptatsiya. In, Sartori, G., Remo, J. and Tressoldi, P. E. (eds.) *DDE-2 Test Battery for Evaluation of Dyslexia of Development.* Bulgaria: OS Bulgaria Ltd. (In Bulgarian)

Mechelli, A., Gorno-Tempini, M. L. and Price, C. J. (2003) Neuroimaging studies of word and pseudoword reading: Consistencies, inconsistencies, and limitations. *Journal of Cognitive Neuroscience* **15**, 260-271.

Medaglia, J. D., Lynall, M. E. and Bassett, D. S. (2015) Cognitive network neuroscience. *Journal of Cognitive Neuroscience* **27**, 1471-1491.

Meyer, L., Obleser, J. and Friederici, A. D. (2013) Left parietal alpha enhancement during working memory-intensive sentence processing. *Cortex* **49**, 711-721.

Michalareas, G., Michalareas, G., Vezoli, J., Van Pelt, S., Schoffelen J. M., Kennedy, H. and Fries, P. (2016) Alpha-beta and gamma rhythms subserve feedback and feedforward influences among human visual cortical areas. *Neuron* **89**, 384-397.

Mizuhara, H. and Yamaguchi, Y. (2007) Human cortical circuits for central executive function emerge by theta phase synchronization. *NeuroImage* **36**, 232-244.

Muldoon, S. F., Bridgeford, E. W. and Bassett, D. S. (2016) Small-world propensity and weighted brain networks. *Scientific Reports* **6**, 22057.

Nikolova, T. S. (1987) *Chestoten rechnik na Balgarski razgovoren ezik. Frequency dictionary of the Bulgarian conversational language.* Bulgaria, Publishing House. (In Bulgarian)

Onnela, J. P., Saramäki, J., Kertész, J. and Kaski, K. (2005) Intensity and coherence of motifs in weighted complex networks. *Physical Review E* **71**, 065103.

Pammer, K. and Wheatley, C. (2001) Isolating the M(y)-cell response in dyslexia using the spatial frequency doubling illusion. *Vision Research* **41**, 2139-2147

Patterson, K. and Hodges, J. R. (1992) Deterioration of word meaning: Implications for reading. *Neuropsychologia* **30,** 1025-1040.

Qian, Y. and Bi, H. Y. (2015) The effect of magnocellular-based visual-motor intervention on Chinese children with developmental dyslexia. *Frontiers in Psychology* **6**, 1529.

Raichev, P., Geleva, T., Valcheva, M., Rasheva, M. and Raicheva, M. (2005) Protokol za nevrologichno i nevropsihologichno izslenvane na detsa sas spetsifichni obuchitelni zatrudneniya. In, Evgenieva, E. (eds.) *Integrated Learning and Resource Teacher (pp. 82-105)*. Bulgaria: Publishing House. (In Bulgarian)

Raven, J., Raven, J. C. and Court, J. H. (1998) *Manual for Raven's progressive matrices and vocabulary scales*. *Section 2: The coloured progressive matrices.* Oxford, UK: Oxford Psychologists Press.

Rice, G. E., Lambon Ralph, M. A. and Hoffman, P. (2015) The roles of left versus right anterior temporal lobes in conceptual knowledge: An ALE meta-analysis of 97 functional neuroimaging studies. *Cerebral Cortex* **25**, 4374-4391.

Ross-Sheehy, S., Oakes, L. M. and Luck, S. J. (2011) Exogenous attention influences visual short-term memory in infants. *Developmental Science* **14**, 490-501.

Rubinov, M. and Sporns, O. (2010) Complex network measures of brain connectivity: Uses and interpretations. *Neuroimage* **52**, 1059-1069.

Sandak, R., Mencl, W. E., Frost, S. J. and Pugh, K. R. (2004) The neurobiological basis of skilled and impaired reading: Recent findings and new directions. *Journal Scientific Studies of Reading* **8**, 273-292.

Sartori, G., Remo, J. and Tressoldi, P. E. (2007) *Updated and Revised Edition for The Evaluation of Dyslexia*. Italy: Giunti Organizzazionioni Speciali.

Sauseng, P., Hoppe, J., Klimesch, W., Gerloff, C. and Hummel, F. C. (2007) Dissociation of sustained attention from central executive functions: Local activity and interregional connectivity in the theta range. *European Journal of Neuroscience* **25**, 587-593.

Sauseng, P., Klimesch, W., Schabus, M. and Doppelmayr, M. (2005) Fronto-parietal EEG coherence in theta and upper alpha reflect central executive functions of working memory. *International Journal of Psychophysiology* **57**, 97-103.

Schoffelen, J. M., Hulten, A., Lam, N., Marquand, A. F., Udden, J. and Hagoort, P. (2017) Frequency-specific directed interactions in the human brain network for language. *Proceedings of the National Academy of Sciences of the United States of America* **114**, 8083-8088.

Siegel, L. S. (1993) The development of reading. In, Reese, H. W. (eds.) *Advances in Child Development And Behavior (pp. 63-97)*. San Diego: Academic Press.

Sperling, A. J., Lu, Z. I., Manis, F. R. and Seidenberg, M. S. (2003) Selective magnocellular deficits in dyslexia: A "phantom contour" study. *Neuropsychologia* **41**, 1422-1429.

Sperling, A. J., Lu, Z. L., Manis, F. R. and Seidenberg, M. S. (2005) Deficits in perceptual noise exclusion in developmental dyslexia. *Nature Neuroscience* **8**, 862-863.

Spironelli, C., Penolazzi, B. and Angrilli, A. (2008) Dysfunctional hemispheric asymmetry of theta and beta EEG activity during linguistic tasks in developmental dyslexia. *Biological Psychology* **77**, 123-31.

Stam, C. J. and van Straaten, E. C. (2012) The organization of physiological brain networks. *Clinical Neurophysiology* **123**, 1067-1087.

Stam, C. J., Nolte, G. and Daffertshofer, A. (2007) Phase lag index: Assessment of functional connectivity from multi channel EEG and MEG with diminished bias from common sources. *Human Brain Mapping* **28**, 1178-93.

Stein, J. (2014) Dyslexia: The role of vision and visual attention. *Current Developmental Disorders Reports* **1**, 267-280.

Taskov, T. and Dushanova, J. (2020) Reading-network in developmental dyslexia before and after visual training. *Symmetry* **12**, 1842.

Tomasello, R., Garagnani, M., Wennekers, T. and Pulvermuller, F. (2017) Brain connections of words, perceptions and actions: A neurobiological model of spatio-temporal semantic activation in the human cortex. *Neuropsychologia* **98**, 111-129.

Tsujimoto, S. (2008) The prefrontal cortex: Functional neural development during early childhood. *The Neuroscientist* **14**, 345-358.

Ursino, M., Cuppini, C. and Magosso, E. (2015) A neural network for learning the meaning of objects and words from a featural representation. *Neural Networks* **63**, 234-253.

van Diessen, E., Numan T., van Dellen, E., van der Kooi, A. W., Boersma, M., Hofman, D., van Lutterveld, R., van Dijk, B. W., van Straaten, E. C. W., Hillebrand, A. and Stam, C. J. (2015) Opportunities and methodological challenges in EEG and MEG resting state functional brain network research. *Clinical Neurophysiology* **126**, 1468-1481.

Vigneau, M., Vigneau, M., Beaucousin, V., Hervé, P. Y., Jobard, G., Petit, L., Crivello, F., Mellet, E., Zago, L., Mazoyer, B. and Tzourio-Mazoyer, N. (2011) What is right-hemisphere contribution to phonological, lexico-semantic, and sentence processing? Insights from a meta-analysis. *Neuroimage* **54,** 577-593.

Vinck, M., Oostenveld, R., van Wingerden, M., Battaglia, F. and Pennartz, C. M. A. (2011) An improved index of phase-synchronization for electrophysiological data in the presence of volume-conduction, noise and sample-size bias. *Neuroimage* **55**, 1548-1565.

von Stein, A. and Sarnthein, J. (2000) Different frequencies for different scales of cortical integration: From local gamma to long range alpha/theta synchronization. *International Journal of Psychophysiology* **38**, 301-313.

Vourkas, M., Micheloyannis, S., Simos, P. G., Rezaie, R., Fletcher, J. M., Cirino, P. T. and Papanicolaou, A. C. (2011) Dynamic task-specific brain network connectivity in children with severe reading difficulties. *Neuroscience Letters* **488**, 123-128.

Vourkas, M., Karakonstantaki, E., Simos, P. G., Tsirka, V., Antonakakis, M., Vamvoukas, M., Stam, C., Dimitriadis, S. and Micheloyannis, S. (2014) Simple and difficult mathematics in children: A minimum spanning tree EEG network analysis. *Neuroscience Letters* **576**, 28-33.

Weiss, S., Mueller, H. M., Schack, B., King, J. W., Kutas, M. and Rappelsberger, P. (2005) Increased neuronal communication accompanying sentence comprehension. *International Journal of Psychophysiology* **57**, 129-141.

Wilmer, J. B., Richardson, A. J., Chen, Y. and Stein, J. F. (2004) Two visual motion processing deficits in developmental dyslexia associated with different reading skills deficits. *Journal of Cognitive Neuroscience* **16**, 528-540.

Xia, M., Wang, J. and He, Y. (2013) BrainNet Viewer: A network visualization tool for human brain connectomics. *PLoS One* **8**, e68910.

Yakimova, R. (2004) *Narusheniya na pismenata rech. Abnormalities of written speech*. Bulgaria: Rommel Publishing House. (In Bulgarian)